

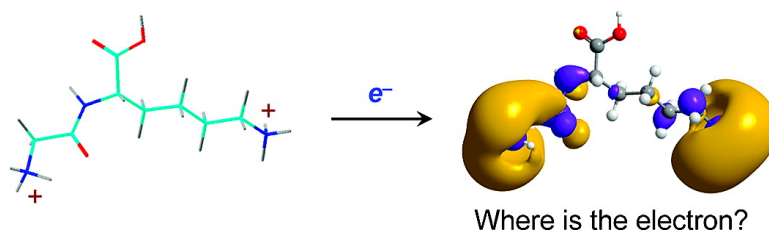
Article

Where Does the Electron Go? Electron Distribution and Reactivity of Peptide Cation Radicals Formed by Electron Transfer in the Gas phase

Frantisek Turecek, Xiaohong Chen, and Changtong Hao

J. Am. Chem. Soc., **2008**, 130 (27), 8818-8833 • DOI: 10.1021/ja8019005 • Publication Date (Web): 14 June 2008

Downloaded from <http://pubs.acs.org> on February 8, 2009



More About This Article

Additional resources and features associated with this article are available within the HTML version:

- Supporting Information
- Access to high resolution figures
- Links to articles and content related to this article
- Copyright permission to reproduce figures and/or text from this article

[View the Full Text HTML](#)

Where Does the Electron Go? Electron Distribution and Reactivity of Peptide Cation Radicals Formed by Electron Transfer in the Gas phase

František Tureček,* Xiaohong Chen,[†] and Changtong Hao[‡]

Department of Chemistry, Bagley Hall, Box 351700, University of Washington, Seattle, Washington 98195-1700

Received March 13, 2008; E-mail: turecek@chem.washington.edu

Abstract: We report the first detailed analysis at correlated levels of ab initio theory of experimentally studied peptide cations undergoing charge reduction by collisional electron transfer and competitive dissociations by loss of H atoms, ammonia, and N–C_α bond cleavage in the gas phase. Doubly protonated Gly-Lys, (GK + 2H)²⁺, and Lys-Lys, (KK + 2H)²⁺, are each calculated to exist as two major conformers in the gas phase. Electron transfer to conformers with an extended lysine chain triggers highly exothermic dissociation by loss of ammonia from the Gly residue, which occurs from the ground (**X**) electronic state of the cation radical. Loss of Lys ammonium H atoms is predicted to occur from the first excited (**A**) state of the charge-reduced ions. The **X** and **A** states are nearly degenerate and show extensive delocalization of unpaired electron density over spatially remote groups. This delocalization indicates that the captured electron cannot be assigned to reduce a particular charged group in the peptide cation and that superposition of remote local Rydberg-like orbitals plays a critical role in affecting the cation-radical reactivity. Electron attachment to ion conformers with carboxyl-solvated Lys ammonium groups results in spontaneous isomerization by proton-coupled electron transfer to the carboxyl group forming dihydroxymethyl radical intermediates. This directs the peptide dissociation toward N–C_α bond cleavage that can proceed by multiple mechanisms involving reversible proton migrations in the reactants or ion–molecule complexes. The experimentally observed formations of Lys z⁺ fragments from (GK + 2H)²⁺ and Lys c⁺ fragments from (KK + 2H)²⁺ correlate with the product thermochemistry but are independent of charge distribution in the transition states for N–C_α bond cleavage. This emphasizes the role of ion–molecule complexes in affecting the charge distribution between backbone fragments produced upon electron transfer or capture.

Introduction

Electron attachment to multiply protonated peptides and proteins has attracted much attention owing to the dissociations of the intermediate cation-radicals that show promise for peptide sequencing,¹ location of post-translational modifications,² and even can be related to the peptide secondary structure.³ Electron

attachment can be realized as capture by a trapped ion of a low-energy electron in electron capture dissociation (ECD),⁴ femtosecond electron transfer to a fast ion from a neutral target⁵ in electron capture induced dissociation (ECID),⁶ or electron transfer from a molecular anion which is trapped together with the peptide cation in electron transfer dissociation (ETD).⁷ All these processes result in the formation of peptide cation radicals that typically undergo efficient dissociation by losses of atoms, neutral molecules, side chain cleavages, and peptide backbone dissociations. The latter typically occur between an amide nitrogen atom and the adjacent C_α position of the C-terminal amino acid residue, the N–C_α cleavage. This bond cleavage is relatively nonselective and forms a series of C_α cation radicals extending from the carboxylate terminus (z⁺ ions) and complementary even-electron cations extending from

[†] Current address: National Institutes of Health (NIH), 9000 Rockville Pike, Bethesda, Maryland 20892.

[‡] Current address: Department of Chemistry, York University, Toronto, Canada.

- (1) (a) Zubarev, R. A.; Horn, D. M.; Fridriksson, E. K.; Kelleher, N. L.; Kruger, N. A.; Lewis, M. A.; Carpenter, B. K.; McLafferty, F. W. *Anal. Chem.* **2000**, *72*, 563–573. (b) Cooper, H. J.; Hakansson, K.; Marshall, A. G. *Mass Spectrom. Rev.* **2005**, *24*, 201–222.
- (2) (a) Stensballe, A.; Jensen, O. N.; Olsen, J. V.; Hasselmann, K. F.; Zubarev, R. A. *Rapid Commun. Mass Spectrom.* **2000**, *14*, 1793–1800. (b) Mirgorodskaya, E.; Roepstorff, P.; Zubarev, R. A. *Anal. Chem.* **1999**, *71*, 4431–4436. (c) Sze, S. K.; Ge, Y.; Oh, H. B.; McLafferty, F. W. *Proc. Natl. Acad. Sci. U.S.A.* **2002**, *99*, 1774–1779. (d) Kelleher, N. L.; Zubarev, R. A.; Bush, K.; Furie, B.; Furie, B. C.; McLafferty, F. W.; Walsh, C. T. *Anal. Chem.* **1999**, *71*, 4250–4253. (e) Ge, Y.; Lawhorn, B. G.; ElNaggar, M.; Strauss, E.; Park, J. H.; Begley, T. P.; McLafferty, F. W. *J. Am. Chem. Soc.* **2002**, *124*, 672–678.
- (3) (a) Breuker, K.; Oh, H. B.; Horn, D. M.; Cerda, B. A.; McLafferty, F. W. *J. Am. Chem. Soc.* **2002**, *124*, 6407–6420. (b) Breuker, K.; Oh, H. B.; Lin, C.; Carpenter, B. K.; McLafferty, F. W. *Proc. Natl. Acad. Sci. U.S.A.* **2004**, *101*, 14011–14016. (c) Robinson, E. W.; Leib, R. D.; Williams, E. R. *J. Am. Soc. Mass Spectrom.* **2006**, *17*, 1469–1479.

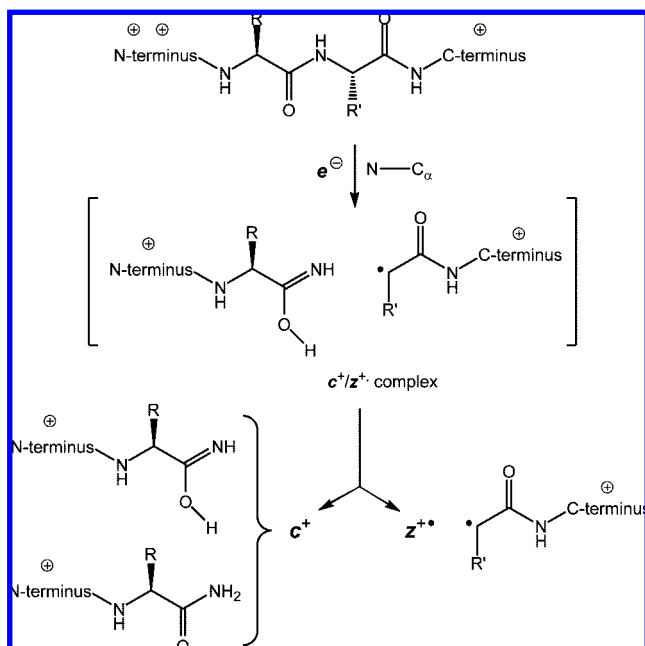
(4) Zubarev, R. A.; Kelleher, N. L.; McLafferty, F. W. *J. Am. Chem. Soc.* **1998**, *120*, 3265–3266.

(5) Tureček, F. *Top. Curr. Chem.* **2003**, *225*, 77–129.

(6) Hvelplund, P.; Liu, B.; Brøndsted Nielsen, S.; Tomita, S. *Int. J. Mass Spectrom.* **2003**, *225*, 83–87.

(7) (a) Syka, J. E. P.; Coon, J. J.; Schroeder, M. J.; Shabanowitz, J.; Hunt, D. F. *Proc. Natl. Acad. Sci. U.S.A.* **2004**, *101*, 9528–9533. (b) Coon, J. J.; Ueberheide, B.; Syka, J. E. P.; Dryhurst, D. D.; Ausio, J.; Shabanowitz, J.; Hunt, D. F. *Proc. Natl. Acad. Sci. U.S.A.* **2005**, *102*, 9463–9468. (c) Pitteri, S. J.; Chrisman, P. A.; Hogan, J. M.; McLuckey, S. A. *Anal. Chem.* **2005**, *77*, 1831–1839.

Scheme 1



the N-terminus (c^+ ions, Scheme 1). The structures of c^+ and z^{++} ions are not known with certainty, although the former are usually represented by enolimine structures, while z^{++} ions are thought to be C α radicals. It is noteworthy that enolimines are substantially less stable than their amide tautomers⁸ and the possibility of exothermic prototropic rearrangement to amides during the dissociation cannot be excluded.

Peptide backbone dissociations and fragment formation have been evaluated empirically for a large set of tryptic peptides.⁹ There has been a lively discussion of the mechanisms pertinent to the N-C α bond cleavage, c^+ and z^{++} fragment separation, and their interactions.^{1,3c,10–18} While the details of the various suggested dissociation mechanisms are beyond the scope of the present study, they share the common feature that the N-C α dissociation is triggered by interaction of the unpaired electron with the valence electrons of the peptide bond framework.¹⁸ Computational analysis of simple amino acid and peptide models established that the N-C α bond was substantially weakened in

radical intermediates following electron attachment.^{16,17,19} For example, aminoketyl radicals, which are produced by electron attachment to the peptide amide bond followed by proton transfer, are metastable with respect to exothermic dissociation of the affected N-C α bond.¹⁷ The dissociations have low activation energies, which are in the range 34–50 kJ mol⁻¹ for peptide radicals from Gly-Gly,¹⁷ Gly-Phe,¹⁹ Gly-Pro, Pro-Gly,²⁰ and Gly-His²¹ and are predicted to proceed with rate constants $> 10^5$ s⁻¹.^{17,19}

A fundamental mechanistic question concerns the electronic structure of the intermediates formed by electron attachment to doubly or multiply protonated peptides. Simons and co-workers have investigated small singly charged amide and disulfide models in which the electron was placed into localized orbitals representing the ground and select excited states of the system.^{22a–c} Cross sections for electron transfer between electronic states localized at distant functional groups were estimated, and effects of distance^{22d,e} and conformation were discussed.^{22f} We have studied by experiment and theory the dissociation energetics and kinetics of several singly charged amino acids²³ and peptide systems²⁴ and pointed out the importance of orbital interactions in dissociations occurring from the ground and excited electronic states.²⁴ In particular, hydrogen atom migrations in peptide cation radicals have been described within the proton-coupled electron transfer model.^{16,25} However, a detailed electronic structure theory analysis of experimentally studied doubly charged peptide ions has been elusive so far.

Recently, a University of Aarhus group reported ECID spectra of doubly protonated dipeptides Gly-Lys, Ala-Lys, and Lys-Lys that showed major competitive dissociations by loss of H, ammonia, and N-C α bond cleavage forming z^{++} ions.²⁶ That study utilized femtosecond electron transfer from alkali metal atoms under predominantly single collision conditions at 100 keV of ion kinetic energy. Isotope labeling established that the ammonia molecule that was eliminated from the cation radicals selectively originated from the N-terminal amino group,²⁷ consistent with our earlier computational analysis of dissociations of a related Gly-Gly-amide system.^{16,17} ECID of doubly

- (8) (a) Syrstad, E. A.; Stephens, D. D.; Tureček, F. *J. Phys. Chem. A* **2003**, *107*, 115–126. (b) Tam, F.; Syrstad, E. A.; Chen, X.; Tureček, F. *Eur. J. Mass Spectrom.* **2004**, *10*, 869–879.
- (9) Savitski, M. M.; Kjeldsen, F.; Nielsen, M. L.; Zubarev, R. A. *Angew. Chem., Int. Ed.* **2006**, *45*, 5301–5303.
- (10) (a) Leymarie, N.; Costello, C. E.; O'Connor, P. B. *J. Am. Chem. Soc.* **2003**, *125*, 8949–8958. (b) O'Connor, P. B.; Lin, C.; Cournoyer, J. J.; Pittman, J. L.; Belyayev, M.; Budnik, B. A. *J. Am. Soc. Mass Spectrom.* **2006**, *17*, 576–585. (c) Lin, C.; O'Connor, P. B.; Cournoyer, J. J. *J. Am. Soc. Mass Spectrom.* **2006**, *17*, 1605–1615.
- (11) Bakken, V.; Helgaker, T.; Uggerud, E. *Eur. J. Mass Spectrom.* **2004**, *10*, 625–638.
- (12) (a) Patriksson, A.; Adams, C.; Kjeldsen, F.; Raber, J.; van der Spoel, D.; Zubarev, R. A. *Int. J. Mass Spectrom.* **2006**, *248*, 124–135. (b) Savitski, M. M.; Kjeldsen, F.; Nielsen, M. L.; Zubarev, R. A. *J. Am. Soc. Mass Spectrom.* **2007**, *18*, 113–120.
- (13) Mihalca, R.; Kleinnijenhuis, A. J.; McDonnell, L. A.; Heck, A. J. R.; Heeren, R. M. A. *J. Am. Soc. Mass Spectrom.* **2004**, *15*, 1869–1873.
- (14) Cooper, H. J. *J. Am. Soc. Mass Spectrom.* **2005**, *16*, 1932–1940.
- (15) Fung, Y. M. E.; Chan, T.-W. D. *J. Am. Soc. Mass Spectrom.* **2005**, *16*, 1523–1535.
- (16) Tureček, F.; Syrstad, E. A. *J. Am. Chem. Soc.* **2003**, *125*, 3353–3369.
- (17) Tureček, F. *J. Am. Chem. Soc.* **2003**, *125*, 5954–5963.
- (18) Syrstad, E. A.; Tureček, F. *J. Am. Soc. Mass Spectrom.* **2005**, *16*, 208–224.

- (19) Tureček, F.; Syrstad, E. A.; Seymour, J. L.; Chen, X.; Yao, C. *J. Mass Spectrom.* **2003**, *38*, 1093–1104.
- (20) Hayakawa, S.; Hashimoto, M.; Matsubara, H.; Tureček, F. *J. Am. Chem. Soc.* **2007**, *129*, 7936–7949.
- (21) Tureček, F. Presented at the 54th Annual Conference of the American Society for Mass Spectrometry, Seattle, WA, May 28–June 1, 2006.
- (22) (a) Sobczyk, M.; Anusiewicz, I.; Berdys-Kochanska, J.; Sawicka, A.; Skurski, P.; Simons, J. *J. Phys. Chem. A* **2005**, *109*, 250–258. (b) Anusiewicz, I.; Berdys-Kochanska, J.; Simons, J. *J. Phys. Chem. A* **2005**, *109*, 5801–5813. (c) Anusiewicz, I.; Berdys-Kochanska, J.; Skurski, P.; Simons, J. *J. Phys. Chem. A* **2006**, *110*, 1261–1266. (d) Sobczyk, M.; Simons, J. *Int. J. Mass Spectrom.* **2006**, *253*, 274–280. (e) Sobczyk, M.; Simons, J. *J. Phys. Chem. B* **2006**, *110*, 7519–7527. (f) Skurski, P.; Sobczyk, M.; Jakowski, J.; Simons, J. *Int. J. Mass Spectrom.* **2007**, *265*, 197–212. (g) Sobczyk, M.; Neff, D.; Simons, J. *Int. J. Mass Spectrom.* **2008**, *269*, 149–164.
- (23) Yao, C.; Syrstad, E. A.; Tureček, F. *J. Phys. Chem. A* **2007**, *111*, 4167–4180.
- (24) Chamot-Rooke, J.; Malosse, C.; Frison, G.; Tureček, F. *J. Am. Soc. Mass Spectrom.* **2007**, *18*, 2146–2161.
- (25) (a) Siegbahn, P. E. M.; Blomberg, M. R. A.; Crabtree, R. H. *Theor. Chim. Acc.* **1997**, *97*, 289–300. (b) Siegbahn, P. E. M.; Eriksso, L.; Himo, F.; Pavlov, M. *J. Phys. Chem. B* **1998**, *102*, 10622–10629. (c) Huyhn, M. H. V.; Meyer, T. *J. Chem. Rev.* **2007**, *107*, 5004–5064.
- (26) Chakraborty, T.; Holm, A. I. S.; Hvelplund, P.; Nielsen, S. B.; Pouilly, J.-C.; Worm, E. S.; Williams, E. R. *J. Am. Soc. Mass Spectrom.* **2006**, *17*, 1675–1680.
- (27) Holm, A. I. S.; Hvelplund, P.; Kadhane, U.; Larsen, M. K.; Liu, B.; Nielsen, S. B.; Panja, S.; Pedersen, J. M.; Skrydstrup, T.; Stochkel, K.; Williams, E. R.; Worm, E. S. *J. Phys. Chem. A* **2007**, *111*, 9641–9643.

charged D₇-Gly-Lys from incomplete exchange of amide and ammonium protons showed competitive loss of H and D.²⁶ In addition, charge distribution between the c⁺ and z⁺⁺ backbone fragments from charge-reduced (Lys-Lys + 2H)⁺⁺ showed an 8:1 preference for the c⁺ ions.²⁶

ECID of Gly-Lys and Lys-Lys has provided an opportunity to apply computational analysis by electronic structure theory to a real system that has been studied under well controlled conditions.^{26,27} Due to the nature of the Aarhus experiments, the incipient cation radicals are formed by vertical electron transfer to the isolated precursor cations on a low femtosecond time scale, and so their initial structures correspond practically exactly to those of the precursor ions.⁵ This greatly simplifies computational analysis because the search of the conformational space is performed for closed shell systems whose conformations are restricted by Coulomb interactions between the charges. Following femtosecond collisional electron transfer, ECID products are formed on the low microsecond time scale, which may limit reactions of the incipient c⁺ and z⁺⁺ in ion–molecule complexes. Last but not least, Gly-Lys and Lys-Lys can be viewed as truncated analogues of tryptic peptides, which are of main interest in proteomic analysis by mass spectrometry. We wish to show that electron attachment to doubly protonated peptides is adequately described by electronic states that ensue from superposition of orbitals at remote functional groups. We believe that the present analysis provides a new paradigm in considering the title question: “Where does the electron go?”.

Calculations

Standard ab initio calculations were performed using the Gaussian 03 suite of programs.²⁸ Optimized geometries were obtained by density functional theory calculations using Becke’s hybrid functional (B3LYP)²⁹ and the 6-31+G(d,p) and 6-31++G(d,p) basis sets for closed-shell and open-shell species, respectively. Select optimized structures are shown in the pertinent schemes and figures. Cartesian coordinates in standard orientation for complete optimized structures of local minima and transition states as well as total energies are given in the Supporting Information. Spin unrestricted calculations were performed for all open-shell systems. Stationary points were characterized by harmonic frequency calculations with B3LYP/6-31+G(d,p) or 6-31++G(d,p) as local minima (all real frequencies) and first-order saddle points (one imaginary frequency). The calculated frequencies were scaled with 0.963³⁰ and used to obtain zero-point energy corrections, enthalpies, and entropies. The rigid-rotor-harmonic-oscillator (RRHO) model was used in thermochemical calculations except for low frequency modes where the vibrational enthalpy terms that exceeded 0.5 RT were replaced by free internal rotation terms equal to 0.5 RT.

Improved energies were obtained by single-point calculations that were carried out with B3LYP and Møller–Plesset theory (second order, frozen core) using the 6-311++G(2d,p) split-valence triple- ζ basis set furnished with polarization and diffuse functions. For the molecular system of the (Lys-Lys + 2H) size, the larger basis set comprised 1050 primitive gaussians and the MP2 calculations required over 50 GByte scratch space. Contamination by higher spin states was modest, as judged from the expectation values of the spin operator $\langle S^2 \rangle$ that were ≤ 0.76 for UB3LYP and ≤ 0.78 for UMP2 calculations. The UMP2 energies were corrected

by spin annihilation³¹ that reduced the $\langle S^2 \rangle$ to close to the theoretical value for a pure doublet state (0.75). Spin annihilation lowered the total MP2 energies by 2.3 millihartrees (6.2 kJ mol⁻¹) for local energy minima and by 7.1 millihartrees (18.8 kJ mol⁻¹) for transition states, both expressed as root-mean-square deviations. The B3LYP and MP2 energies calculated with the large basis set were combined according to the B3-MP2 scheme (eq 1), as described previously.³²

$$E[\text{B3-MP2}/6-311++\text{G}(2\text{d},\text{p})] = 0.5\{E[\text{B3LYP}/6-311++\text{G}(2\text{d},\text{p})] + E[\text{PMP2}/6-311++\text{G}(2\text{d},\text{p})]\} \quad (1)$$

This scheme is based on the observation^{32a} that, for a number of closed-shell and open-shell electronic systems, B3LYP and MP2 calculations with triple- ζ basis sets provide relative, reaction, and transition state energies that differ from the benchmark values by a similar magnitude but in an opposite sense. Averaging the relative energies results in efficient error cancellation, and the B3-MP2 relative energies have been shown to favorably compare to those obtained by coupled-cluster or Gaussian-type composite single-point calculations.^{32b–d} The theoretical basis for this observation can be found in the analysis of H₂ dissociation where B3LYP overestimates the correlation energy, while MP2 underestimates it by the same amount when compared to full-CI reference calculations.³³

Vertical excited-state energies were calculated with time-dependent density functional theory³⁴ using the B3LYP functional and the 6-311++G(2d,p) basis set. Atomic spin and charge densities were calculated using the Natural Population Analysis (NPA) method.³⁵ Excited state wave functions were constructed as linear combinations of virtual orbitals with expansion coefficients obtained from TD-B3LYP/6-311++G(2d,p) calculations. Unimolecular rate constants were calculated according to the Rice–Ramsperger–Kassel–Marcus theory³⁶ using Hase’s program³⁷ that was recompiled and run under Windows XP.³⁸ Rotational states were treated adiabatically, and microcanonical rate constants, $k(E,J,K)$, were calculated with a direct count of quantum states in 2 kJ mol⁻¹ steps from the transition state energy up to 300–400 kJ mol⁻¹ above it. The rate constants at each internal energy point were averaged over the Boltzmann distribution of rotational states at 298 K, corresponding to the ambient temperature of the electrospray ion source of the Aarhus instrument.⁶ RRKM calculations on B3-MP2 potential energy surfaces have been shown to give relative rate constants and branching ratios that agreed within 20% with experimental data for various radical systems.^{8a,32c}

Results

(GK + 2H)²⁺ Ion Structures and Relative Stabilities. The protonation sites in GK can be unequivocally assigned to the N-terminal and Lys amino groups, which are the most basic

(28) Frisch, M. J. et al. *Gaussian 03*, revision B.05; Gaussian, Inc.: Pittsburgh, PA, 2003.

(29) (a) Becke, A. D. *J. Chem. Phys.* **1993**, *98*, 1372–1377. (b) Becke, A. D. *J. Chem. Phys.* **1993**, *98*, 5648–5652. (c) Stephens, P. J.; Devlin, F. J.; Chabalowski, C. F.; Frisch, M. J. *J. Phys. Chem.* **1994**, *98*, 11623–11627.

(30) Rauhut, G.; Pulay, P. *J. Phys. Chem.* **1995**, *99*, 3093–3100.

(31) (a) Schlegel, H. B. *J. Chem. Phys.* **1986**, *84*, 4530–4534. (b) Mayer, I. *Adv. Quantum Chem.* **1980**, *12*, 189–262.

(32) (a) Tureček, F. *J. Phys. Chem. A* **1998**, *102*, 4703–4713. (b) Tureček, F.; Poláček, M.; Frank, A. J.; Sadílek, M. *J. Am. Chem. Soc.* **2000**, *122*, 2361–2370. (c) Poláček, M.; Tureček, F. *J. Am. Chem. Soc.* **2000**, *122*, 9511–9524. (d) Tureček, F.; Yao, C. *J. Phys. Chem. A* **2003**, *107*, 9221–9231. (e) Rablen, P. R. *J. Am. Chem. Soc.* **2000**, *122*, 357–368. (f) Rablen, P. R. *J. Org. Chem.* **2000**, *65*, 7930–7937. (g) Rablen, P. R.; Bentrup, K. H. *J. Am. Chem. Soc.* **2003**, *125*, 2142–2147. (h) Hiram, M.; Tokosumi, T.; Ishida, T.; Aihara, J. *J. Chem. Phys.* **2004**, *305*, 307–316.

(33) Rassolov, V. A.; Ratner, M. A.; Pople, J. A. *J. Chem. Phys.* **2000**, *112*, 4014–4019.

(34) Stratmann, R. E.; Scuseria, G. E.; Frisch, M. J. *J. Chem. Phys.* **1998**, *109*, 8218.

(35) Reed, A. E.; Weinstock, R. B.; Weinhold, F. *J. Chem. Phys.* **1985**, *83*, 735–746.

(36) Gilbert, R. G.; Smith, S. C. *Theory of Unimolecular and Recombination Reactions*; Blackwell Scientific Publications: Oxford, 1990; 52–132.

(37) Zhu, L.; Hase, W. L. *Quantum Chemistry Program Exchange*; Indiana University: Bloomington, IN, 1994; Program No. QCPE 644.

(38) Frank, A. J.; Sadílek, M.; Ferrier, J. G.; Tureček, F. *J. Am. Chem. Soc.* **1997**, *119*, 12343–12353.

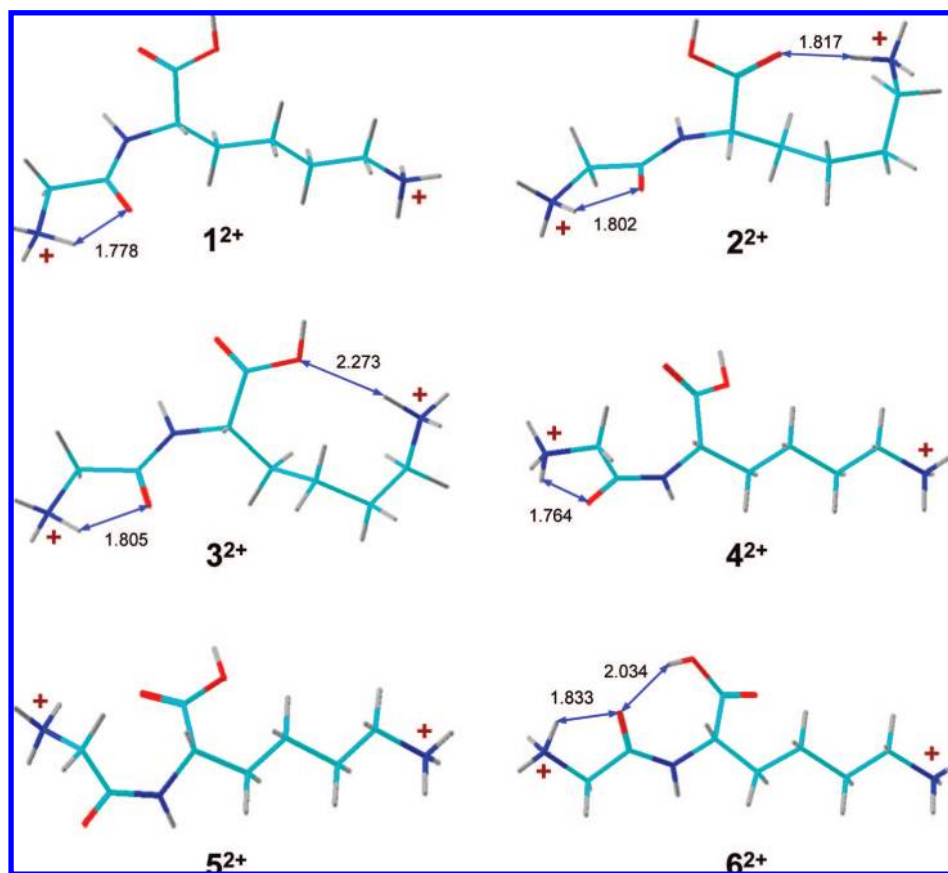


Figure 1. B3LYP/6-31+G(d,p) optimized structures of (GK + 2H)²⁺ cations **1**²⁺–**6**²⁺. The atoms are color-coded as follows: Turquoise, C; blue, N; red, O; gray, H. Hydrogen bonds are indicated by blue double arrows, and the distances are given in angstroms.

Table 1. Relative Energies of (GK + 2H)²⁺ Cations

conformer	relative energy ^a	
	B3LYP/ 6-31+G(d,p)	B3-MP2/ 6-311++G(2d,p)
1 ²⁺	0	0 (0.0) ^b
2 ²⁺	–6.5	–6 (0.6)
3 ²⁺	22	19 (25)
4 ²⁺	24	24 (26)
5 ²⁺	28	26 (30)
6 ²⁺	37	34 (35)

^a Relative enthalpies in units of kJ mol^{–1} including B3LYP/6-31+G(d,p) zero-point energy corrections and 298 K enthalpies.

^b Values in parentheses are relative free energies at 298 K.

sites in the gas-phase molecule.³⁹ Several conformers were investigated for doubly protonated GK dipeptides that differed in hydrogen bonding between the ammonium groups and the carboxylate or amide groups. The six lowest-energy conformers are shown in Figure 1. Structures **1**²⁺ and **2**²⁺ are practically isoenergetic at the present high level of theory (Table 1). **1**²⁺ has the Gly ammonium H-bonded to the amide carbonyl, whereas the Lys chain is fully extended. The distance between the ammonium N atoms in **1**²⁺ is 10.0 Å. **2**²⁺ also has the Gly ammonium H-bonded to the amide carbonyl, whereas the Lys chain is folded and its ammonium is H-bonded to the carbonyl oxygen of the carboxyl group. The distance between the ammonium N atoms in **1**²⁺ is 9.3 Å. The increased Coulomb repulsion between the charged groups in **2**²⁺ is overcompensated

by intramolecular H bonding of the Lys ammonium. While **2**²⁺ is slightly more stable than **1**²⁺ thermochemically, $\Delta H_{g,298}^{\circ}(\mathbf{1}^{2+} \rightarrow \mathbf{2}^{2+}) = -6 \text{ kJ mol}^{-1}$ (Table 1), it has a lower entropy due to the restricted rotation of the folded Lys side chain. The calculated $\Delta G_{g,298}^{\circ}(\mathbf{1}^{2+} \rightarrow \mathbf{2}^{2+}) = 0.6 \text{ kJ mol}^{-1}$ (Table 1) indicates a 56/44 ratio for **1**²⁺/**2**²⁺ at thermal equilibrium at 298 K. We note that interconversions of ion conformers by side-chain rotations have activation energies on the order of 7–15 kJ mol^{–1} and therefore are fast ($k > 10^9 \text{ s}^{-1}$) even at room temperature in the gas phase. This justifies considerations of conformer equilibrium on the microsecond flight time scale for precursor ions in the ECID measurements. The other (GK + 2H)²⁺ conformers (**3**²⁺–**6**²⁺, Figure 1) are $\geq 25 \text{ kJ mol}^{-1}$ less stable than **1**²⁺ and **2**²⁺ and are not expected to be significantly populated in the gas phase at 298 K.

The calculations indicate that the ion populations which are sampled for femtosecond electron transfer consist of two major components, which upon electron transfer give rise to two distinct populations of charge-reduced cation radicals. The cross sections for collisional electron transfer from alkali metal atoms may depend on the precursor ion structure, and so the populations of charge-reduced ions may differ from those of **1**²⁺ and **2**²⁺. However, the differences in electron transfer cross sections are not expected to be large for isomers,^{5,6} and therefore cation radicals formed from both **1**²⁺ and **2**²⁺ have to be considered as reactants in further unimolecular dissociations. We will show that the electronic properties and reactivity of charge reduced **1**²⁺ and **2**²⁺ differ very substantially and that these differences critically affect their reactivity.

(39) Harrison, A. G. *Chemical Ionization Mass Spectrometry*, 2nd ed.; CRC Press: Boca Raton, FL, 1992.

Table 2. Dissociation and Transition State Energies for (GK + 2H)⁺⁺ Cation Radical 1⁺⁺

species/reaction	relative energy ^{a,b}	
	B3LYP/ 6-31++G(d,p)	B3-PMP2/ 6-311++G(2d,p)
1 ²⁺ → 1 ⁺⁺	-590	-557 (5.77) ^c
1 ²⁺ → 1 ⁺⁺ (vertical)	-566	-538 (5.58) ^d
2 ²⁺ → 2 ⁺⁺ (vertical)	-561	-531 (5.50) ^d
4 ²⁺ → 4 ⁺⁺ (vertical)	-570	-545 (5.65) ^d
1 ⁺⁺ → TS1	8	3
1 ⁺⁺ → 1a ⁺⁺	-198	-223
1 ⁺⁺ → 1b ⁺⁺ + NH ₃	-157	-181
1 ⁺⁺ → TS2	25	27
1 ⁺⁺ → TS3	-132	-156
1 ⁺⁺ → 1c ⁺⁺ + NH ₃	-87	-112
1 ⁺⁺ → TS4	36	15
1 ⁺⁺ → 1d ⁺ + H [•]	20	-20
1 ⁺⁺ → 1e ⁺ + H [•]	-27	-65
1 ⁺⁺ → TS5	2.5	15
1 ⁺⁺ → 1f ⁺⁺	-29	-51
1 ⁺⁺ → TS6	0	-17
1 ⁺⁺ → TS7	5	7
1 ⁺⁺ → TS8	13	12
1 ⁺⁺ → TS9	11	11
1 ⁺⁺ → TS10	13	12
1 ⁺⁺ → 1g ⁺⁺	-71	-93
1 ⁺⁺ → TS11	-70	-86
1 ⁺⁺ → 1h ⁺⁺	-141	-154
1 ⁺⁺ → TS12	-73	-96
1 ⁺⁺ → 1i ⁺⁺	-92	-116
1 ⁺⁺ → TS13	-42	-61
1 ⁺⁺ → 1j ⁺⁺	-211	-220
1 ⁺⁺ → c1 + z1 ⁺⁺	-80	-90
1 ⁺⁺ → c2 + z1 ⁺⁺	-156	-161
1 ⁺⁺ → c1 ⁺ + z1 [•]	-12	0
1 ⁺⁺ → c2 ⁺ + z1 [•]	-80	-90

^a In units of kJ mol⁻¹. ^b From B3-PMP2/6-311++G(2d,p) single-point calculations including B3LYP/6-31++G(d,p) zero-point vibrational energies and referring to 0 K. ^c Adiabatic recombination energies in eV. ^d Vertical recombination energies in eV.

Electron Transfer to 1²⁺. Electron capture by 1²⁺ is associated with a vertical recombination energy of $RE_v = 5.58$ eV (Table 2) to reach the ground electronic state of the charge-reduced cation radical. This is slightly greater than the ionization energy of Na (5.139 eV), indicating that collisional electron transfer from Na is exothermic by $\Delta E = |5.14 - 5.58| = 0.44$ eV (42 kJ mol⁻¹). Hereinafter, the recombination energies are given as absolute values. The charge-reduced cation (1⁺⁺) exists in a potential energy minimum, and its equilibrium geometry (Figure 2) does not differ much from that of the 1²⁺ precursor ion. The main difference is the weaker H-bond of the Gly ammonium to the amide carbonyl in 1⁺⁺, as expressed by a longer N–H...O=C distance (Figure 2). The adiabatic recombination energy for 1²⁺ → 1⁺⁺ is $RE_a = 5.77$ eV (Table 2). The difference between RE_a and RE_v (0.19 eV = 18 kJ mol⁻¹) gives an estimate of vibrational excitation in 1⁺⁺ due to Franck–Condon effects after the cation radical has relaxed to its equilibrium geometry.⁵ When combined with the rovibrational enthalpy of the precursor cation 1²⁺ (33 kJ mol⁻¹ at 298 K), 1⁺⁺ formed by electron transfer from Na is estimated to have a mean internal energy of 42 + 33 = 75 kJ mol⁻¹.⁴⁰ This corresponds to an effective temperature of 410 K.⁴¹

The electronic state manifold in vertically formed 1⁺⁺ is shown in Figure 3 for the six lowest states (*X* through *E*). Also

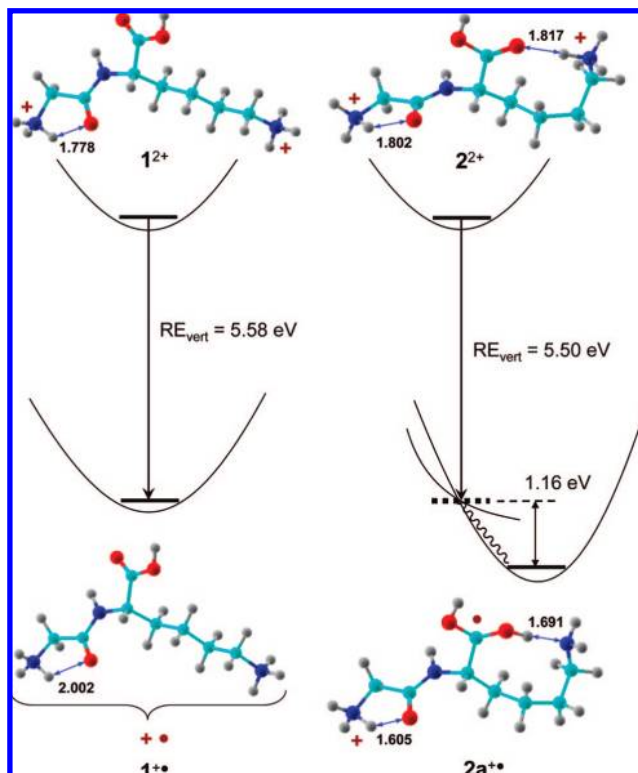


Figure 2. Energy diagram for vertical and adiabatic electron attachment to 1²⁺ and 2²⁺. The recombination and excitation energies are in eV.

shown is the highest doubly occupied molecular orbital (MO, 55αβ), which is an amide π orbital lying 6.44 eV below the *X* state energy. The excitation energy for electron promotion from the amide π orbital to the singly occupied orbital (6.44 eV) is greater than the binding energy of the unpaired electron in the *X* state (5.77 eV). This indicates that electron transfer from Na (or any other electron donor) cannot result in excitation of the paired valence electrons to give a bound state, because states accessed by such excitation would be autoionizing and thus unstable. Bound electronic states in 1⁺⁺ can result only from single electron excitation from the *X* state or by direct electron placement into an excited state.

The *X* and *A* states in vertically formed 1⁺⁺ are closely spaced, $\Delta E_{exc}(X \rightarrow A) = 0.12$ eV, but differ substantially in the electron density distribution. The *X* state has the electron density distributed in two separate regions, one around the Lys ammonium and the other around the Gly ammonium. The singly occupied molecular orbital (SOMO) of the *X* state can be characterized as a constructive superposition of 3s Rydberg-like molecular orbitals located at the ammonium groups with minor contributions of carbonyl π*-orbitals. This is substantiated by the calculated (NPA) unpaired electron densities, which place 61% of spin density at atoms of the incipient *z* fragment in the Lys residue and 39% at atoms in the incipient *c* fragment from the Gly residue. Thus, the electron is delocalized over spatially remote ammonium groups in the *X* state. This indicates that *the question of where the electron goes cannot be answered by assigning an unpaired electron to any particular charged group in the precursor cation.* The *A* state shows predominant electron density in a 3s Rydberg-like MO, which is primarily localized at the Lys ammonium. The low-lying *B* and *C* states are combinations of amide and carboxyl π* orbitals, which are analogous to those obtained previously for amide and amino acid models.¹⁸

(40) Tureček, F. *Int. J. Mass Spectrom.* **2003**, *227*, 327–338.

(41) Estimated from the temperature-dependent rotational and vibrational heat capacity of 1⁺⁺.

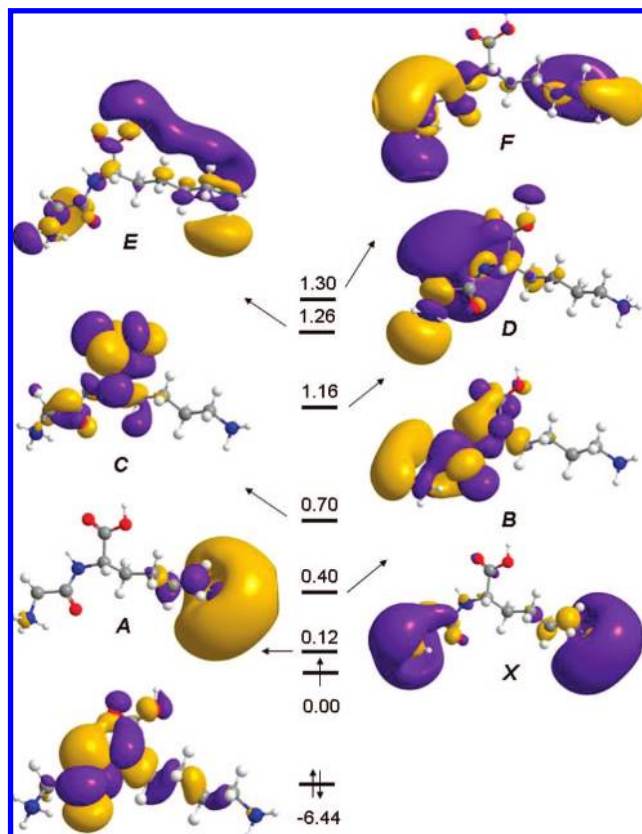


Figure 3. Electronic states in vertically reduced 1^{++} . The energies (eV) are relative to the ground (X) state. The molecular orbitals for excited states were obtained as linear combinations of virtual orbitals with expansion coefficients from TD-B3LYP/6-311++G(2d,p) calculations. The orbitals are drawn as 2% contours so they include 98% of the wave function.

Relaxation of molecular geometry to the local minimum of 1^{++} results in only a minor reorganization of electron density in the ground and low-lying excited states. The pertinent electronic state manifold is shown in Figure 4. The X and A states are near degenerate and correspond to a positive and negative combination, respectively, of Gly and Lys ammonium 3s Rydberg-like orbitals. The unpaired electron density in the X state is distributed at 53% in the incipient z fragment at the Lys residue and 47% in the incipient c fragment from the Gly residue. Again, the electron is delocalized in two spatially distant regions and cannot be specifically assigned to either ammonium group. The B and C states in relaxed 1^{++} are combinations of amide and carboxyl π^* orbitals as in the vertically formed species. The D and E states are Lys ammonium 3p Rydbergs, which however do not mix with 3p orbitals of the Gly ammonium group, because the latter are at higher energies.

We have further pursued the question of electron distribution in a larger system with more remote Gly and Lys ammonium groups as in $(GGK + 2H)^{++}$, where the N...N distance is 13.2 Å in the optimized structure. The results of electronic state analysis are quite analogous to that for 1^{++} (Figure S1, Supporting Information). In particular, the X and A states are practically degenerate ($\Delta E_{\text{exc}}(X \rightarrow A) = 0.06$ eV) and are represented by positive and negative combinations, respectively, of N-terminal Gly and C-terminal Lys ammonium 3s Rydberg-like orbitals. The unpaired electron densities are 35% and 65% in the N-terminal Gly and C-terminal Lys residues, respectively, indicating that the unpaired electron can be specifically assigned to neither charged group in the X state. The analysis of the

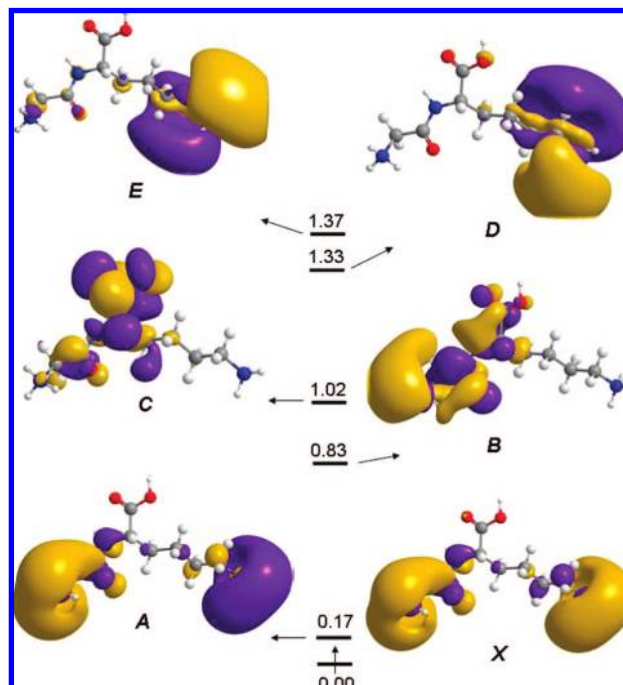


Figure 4. Electronic states in relaxed 1^{++} . The energies (eV) are relative to the ground (X) state.

electronic structure in GK and GGK cation radicals suggests that electron delocalization over remote groups can also be expected for larger charge-reduced peptide cation radicals studied by ECD and ETD. The necessary condition for such delocalization is that the charged groups have similar intrinsic recombination energies, which is satisfied for the typical charged groups in peptides, such as His imidazolium,⁴² Arg guanidinium,^{24,43,44} and Lys ammonium.^{16,17} We note that O-protonated amides have recombination energies that are ~ 0.5 eV higher than those of ammonium groups, and the π orbitals in aminoketyl radicals produced upon electron capture can be expected to be localized within the amide group.¹⁷

Dissociation Energetics of 1^{++} . Several dissociation and isomerization pathways starting from the X state of 1^{++} were investigated, and transition states were located for loss of ammonia from Gly and Lys, loss of an H atom from the Lys ammonium, H-atom migration in the Gly residue, and folding of the Lys side chain.

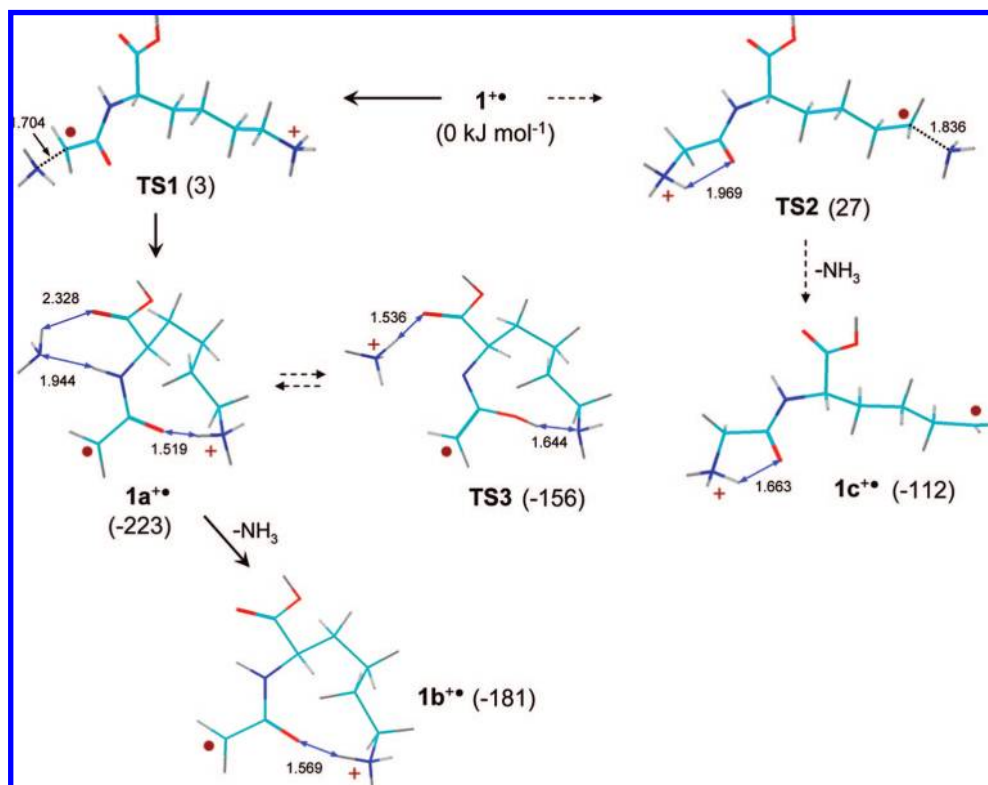
Dissociation of the N-terminal H_3N-CH_2 bond has an extremely low transition state energy in TS1 (Table 2) and results in a highly exothermic dissociation to form an ion-molecule complex ($1a^{++}$) of the incipient product ($1b^{++}$) and ammonia (Scheme 2). TS1 is an early transition state in which the dissociating N-C bond has been elongated by only 13% from the equilibrium bond length of 1.511 Å in 1^{++} and rotated 48° away from the Gly amide plane. The H_3N-C bond cleavage is accompanied by a shift of electron density to the Gly residue, which accounts for 63% of the atomic spin density in TS1 with most of it being delocalized over the CH_2CON moiety. The electron density distribution in ion-molecule complex $1a^{++}$ suggests it to be a distonic ion,⁴⁵ in which the spin density is contained 99% within the CH_2CON group, while

(42) Nguyen, V. Q.; Tureček, F. *J. Mass Spectrom.* **1996**, *31*, 1173–1184.

(43) Chen, X.; Tureček, F. *J. Am. Chem. Soc.* **2006**, *128*, 12520–12530.

(44) Hayakawa, S.; Matsubara, H.; Panja, S.; Hvelplund, P.; Nielsen, S. B.; Chen, X.; Tureček, F. *J. Am. Chem. Soc.* **2008**, *130*.

Scheme 2



the positive charge resides in the Lys ammonium group and side chain. The overall dissociation of $1^{+•} \rightarrow 1b^{+•} + NH_3$ is 181 kJ mol⁻¹ exothermic (Table 2).

A subtle feature of the previous experiments was the ~1:1 ratio for loss of ND_3 and ND_2H upon ECID of D_7 -(GK + $2H$)²⁺.²⁶ Although the experimental ratio is not far from that for statistically random eliminations of ND_3 and ND_2H , $[ND_3]/[ND_2H] = 5:3$, we investigated the possibility of an enhanced loss of ND_2H by H/D exchange of ND_3 with the backbone amide proton in a dissociation intermediate. If complete, such an exchange would favor loss of ND_2H over $[ND_3]$ by a 3:1 ratio, and so even partial exchange could contribute to the enhanced formation of ND_2H . A transition state for H/D exchange in complex $1a^{+•}$ was indeed found (TS3, Scheme 2), which was a complex of the ammonium ion (NH_4^+) that was H-bonded to the carboxyl group of the radical counterpart. Abstraction of the amide proton by the ammonia molecule increases the intrinsic basicity of the amide group and drives a concomitant proton migration from the Lys ammonium to the amide oxygen in TS3. However, TS3 is 67 kJ mol⁻¹ above $1a^{+•}$ and 25 kJ mol⁻¹ above the dissociation threshold for loss of NH_3 to form $1b^{+•}$. With regard to this energy difference and the nature of these two reactions (rearrangement versus dissociation by fragment separation), it appears that H/D exchange in $1a^{+•}$ should be kinetically disfavored. The experimental 1:1 ratio for ND_3 and ND_2H elimination is probably due to secondary isotope effects that slightly favor loss of ND_2H over the 37.5% statistical fraction. Loss of ammonia from the lysine NH_3 group has a TS

energy (TS2), which is substantially higher than TS1 although it also results in an exothermic dissociation to form $1c^{+•}$ (Scheme 2).

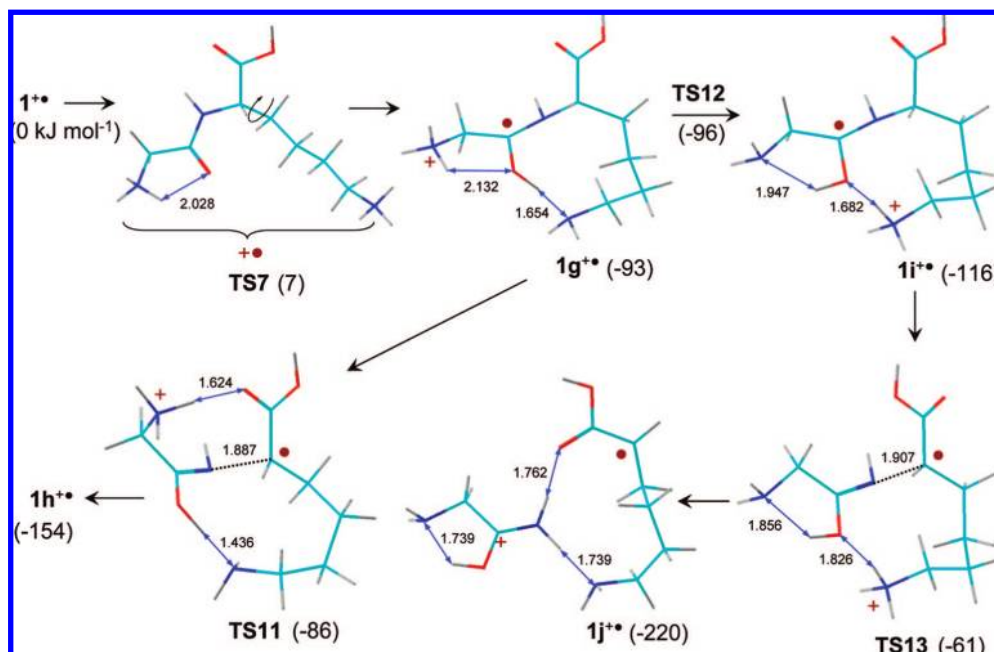
Loss of an H atom is another important dissociation of charge-reduced (GK + H)^{+•} that can proceed from either ammonium group. Loss of H from Lys has a low activation energy in TS4 and is overall mildly exothermic to form a Gly-protonated Gly-Lys fragment ($1d^+$) (Scheme 3, Table 2). The latter may spontaneously isomerize to a more stable Lys-protonated tautomer, such as $1e^+$.

Cleavage of the peptide $N-C_\alpha$ bond in $1^{+•}$ can be triggered by a proton migration from the Gly-ammonium to the amide oxygen in the Lys-extended conformer forming aminoketyl radical $1f^{+•}$ (Scheme 4). The $1^{+•} \rightarrow 1f^{+•}$ isomerization is 51 kJ mol⁻¹ exothermic and overcomes a 15 kJ mol⁻¹ barrier in TS5 (Table 2). The subsequent $N-C_\alpha$ bond cleavage in $1f^{+•}$ requires 34 kJ mol⁻¹ in TS6, which is 17 kJ mol⁻¹ below $1^{+•}$ and also below TS5. Therefore, TS5 is the rate-determining step for a $N-C_\alpha$ bond cleavage proceeding through the $1^{+•} \rightarrow TS5 \rightarrow 1f^{+•} \rightarrow TS6$ pathway.

Although TS5 is a low-lying transition state, intermediate $1f^{+•}$ is quite obviously not the most stable aminoketyl isomer, because it lacks H-bonding between the charged Lys ammonium group and a suitable carbonyl electron donor. Therefore, we investigated alternative pathways for the amide \rightarrow aminoketyl isomerization. This can be accomplished by Lys side-chain rotations that can follow multiple pathways depending on the sequence of rotations about the $C_\alpha-C_\beta$, $C_\beta-C_\gamma$, $C_\gamma-C_\delta$, and $C_\delta-C_\epsilon$ bonds. All these rotations have low activation energies which are in the range 7–12 kJ mol⁻¹, as studied for TS7–TS10. Interestingly, rotations about the $C_\beta-C_\gamma$, $C_\gamma-C_\delta$, and $C_\delta-C_\epsilon$ bonds (TS8–TS10, Supporting Information) involve gauche conformer intermediates with Lys ammonium groups,

(45) (a) Yates, B. F.; Bouma, W. J.; Radom, L. *Tetrahedron* **1986**, *42*, 6225–34. (b) Hammerum, S. *Mass Spectrom. Rev.* **1988**, *7*, 123–202. (c) Stirik, K. M.; Kiminkinen, L. K. M.; Kenttamaa, H. I. *Chem. Rev.* **1992**, *92*, 1649–65.

Scheme 5



the $1^{+\bullet} \rightarrow 1j^{+\bullet}$ isomerization ($\Delta H_{\text{rxn}} = -220 \text{ kJ mol}^{-1}$) and the fact that the threshold energy for the formation of the $z1^{+\bullet}$ and $c1$ or $c2$ and fragments is 90 and 161 kJ mol^{-1} , respectively, below $1^{+\bullet}$ (Table 2). Note however, that since **TS11**–**TS13** and the product energy threshold lie way below **TS7**, the latter is expected to be the rate-determining step for the overall N–C α bond dissociation pathway leading to the $z1^{+\bullet}$ fragment ion.

Dissociation Kinetics of $1^{+\bullet}$. Analysis of the potential energy surface for the dissociations and isomerizations of $1^{+\bullet}$ revealed several pathways of low activation energies that led to losses of H, ammonia, and formation of c and $z^{+\bullet}$ fragments. These pathways are potentially competitive depending on the pertinent unimolecular rate constants. These were calculated by RRKM using the B3-PMP2/6-311++G(2d,p) transition state energies including zero-point corrections and are plotted as $\log k$ (s^{-1}) in Figure 5. The RRKM rate constants for all dissociations of

$1^{+\bullet}$ show a steep increase with the reactant internal energy and reach or exceed the dissociation limit, $k = 1/\tau$, where $\tau = 5 \mu\text{s}$ is the experimental lifetime, within $<30 \text{ kJ mol}^{-1}$. Given the vibrational excitation in $1^{+\bullet}$ by vertical electron transfer (75 kJ mol^{-1} , vide supra), the RRKM rate constants are expected to be $>10^{10} \text{ s}^{-1}$ for most dissociations, which is perfectly consistent with the absence of nondissociating charge-reduced $(\text{GK} + 2\text{H})^{+\bullet}$ in the ECID spectra obtained on the 5 μs time scale. Loss of Gly ammonia predominates over a broad range of internal energies in $1^{+\bullet}$, including the interval about 75 kJ mol^{-1} , which is likely to be accessed by electron transfer from Na. In particular, loss of ammonia from Gly is calculated to outcompete that from Lys by >2 orders of magnitude for most of the internal energy range. This conclusion from our RRKM calculations is consistent with the results of previous ^{15}N labeling experiments, which showed $>95\%$ specificity for the elimination of the N-terminal ammonia.²⁷ The RRKM rate constants also indicate that Lys side chain rotations that can trigger exothermic prototropic isomerizations and N–C α bond dissociations are $>10^2$ fold slower than loss of the Gly ammonia over the entire energy interval. Thus according to our analysis, conformer $1^{+\bullet}$ is not expected to significantly contribute to the formation of the $z^{+\bullet}$ fragment ions.

Loss of Lys H atom is the best competitor to the loss of Gly ammonia, and the pertinent $\log k$ curves converge at high internal energies (Figure 5). However, within the internal energy interval about 75 kJ mol^{-1} , loss of ammonia is predicted to outcompete loss of H by at least a factor of 10. This result is not consistent with the ECID spectra where fragment ions from loss of H and ammonia have very similar relative intensities. We note that loss of Lys ammonia H can be accelerated by quantum tunneling through the barrier in **TS3**.¹⁶ H-atom loss can also start from the *A*, *D*, or *E* electronic states of vertically reduced $1^{+\bullet}$, which all have high spin density in the Lys ammonium group (Figure 3). Alkyl ammonium radicals are

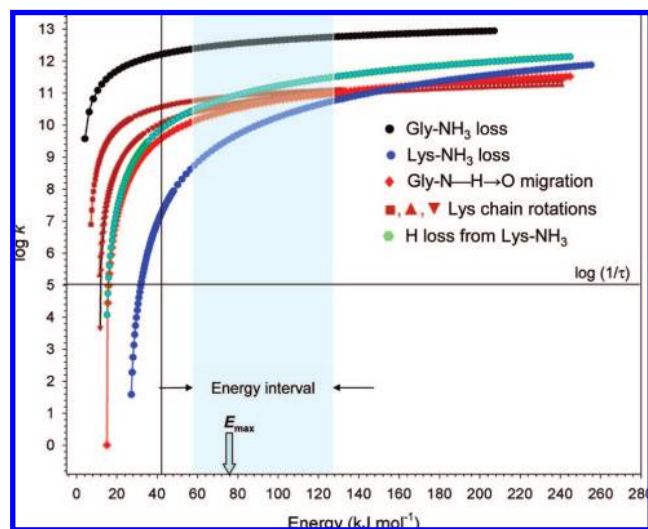
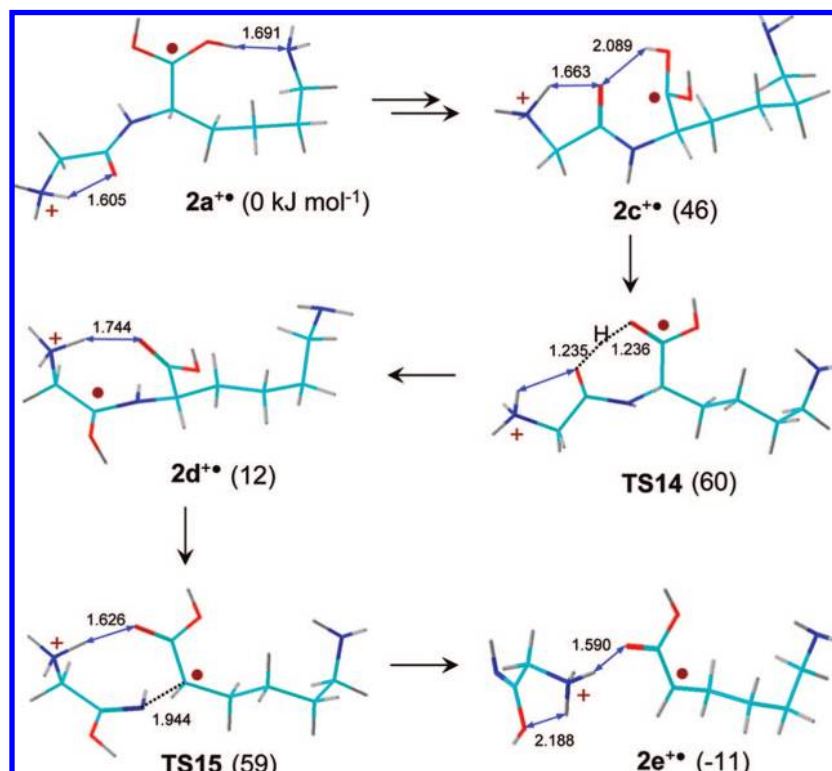


Figure 5. RRKM rate constants ($\log k$, s^{-1}) for dissociations of $1^{+\bullet}$. The gray-shaded area represents the energy interval likely to be populated upon electron transfer from Na.

Scheme 6



known to undergo fast dissociations by loss of H,⁴⁶ which is caused by N–H bond weakening due to an unpaired electron in the 3s Rydberg orbital of the ammonium group.^{46f,g} A similar effect can contribute to the formation of the pertinent fragments from $1^{+\bullet}$ where vibrational excitation tends to increase the electron density at the Lys ammonium by enhancing the 3s Rydberg character of the *A* state. The *A* state is very close to the *X* state in $1^{+\bullet}$ ($\Delta E = 0.17$ eV = 16 kJ mol⁻¹) as well as in **TS3** and so their ro-vibrational envelopes substantially overlap. The transition state for the H-loss from the Lys ammonium is practically isoenergetic with the *A* state, which suggests the possibility of a fast loss of H originating from the *A* state. We conclude that the experimentally observed competitive losses of H and NH₃ occur on different, albeit interacting, potential energy surfaces of $1^{+\bullet}$ and point to the involvement of at least two electronic states accessed by vertical electron transfer from Na.

Electron Transfer to 2^{2+} and Dissociations of 2^{2+} . Cation 2^{2+} is the other major conformer of doubly protonated GK, and charge-reduced intermediates derived from 2^{2+} are expected to play a role in dissociations following electron capture or transfer. Vertical electron capture by 2^{2+} is associated with $RE_v = 5.50$ eV (Table 2), so that vertical electron transfer to 2^{2+} from Na is 0.36 eV exothermic. In contrast to $1^{+\bullet}$, the cation radical formed by electron attachment to 2^{2+} is not a local energy minimum in its *X* electronic state and collapses by migration of a Lys ammonium proton to the carboxyl group. This

barrierless rearrangement is highly exothermic and results in >110 kJ mol⁻¹ vibrational excitation in the pertinent intermediate (Figure 2). The reason for the collapse is the high electron density in the π^* orbital of the COOH group upon vertical electron attachment to the *X*, *A*, and *C* electronic states, which drives the exothermic proton migration. Analogous proton migrations were considered previously in the amide-superbase mechanism of ECD.¹⁸ We note that rearrangements in protonated C-terminal lysine residues upon electron capture have been indicated for other peptides²⁴ and appear to be of a general nature. The spontaneous proton migration forms intermediates that have the unpaired electron 99% contained in the Lys dihydroxymethyl group, whereas the charge is mainly (70%) in the protonated Gly residue.

Several structures for charge-reduced 2^{2+} were obtained as local energy minima that had similar energies and differed in dihedral angles about the N–C_α and C_α–C(OH)₂ as well as Lys side-chain bonds. Such conformers can interconvert through transition states that require much less energy than that received by excitation from vertical electron transfer (vide supra). Structures $2a^{+\bullet}$ and $2b^{+\bullet}$ are representative and are used as starting points for the dissociation pathways.

The first pathway (Scheme 6) starts with cation-radical $2a^{+\bullet}$, which isomerizes to aminoketyl $2d^{+\bullet}$ by C(OH)₂ group rotation ($2c^{+\bullet}$) and H-atom migration (**TS14**). N–C_α cleavage in the latter proceeds through **TS15** and leads to ion–molecule intermediate $2e^{+\bullet}$, which is 11 kJ mol⁻¹ below $2a^{+\bullet}$. The pertinent isomerization and TS energies (Table 3) are ≤ 60 kJ mol⁻¹ relative to $2a^{+\bullet}$ and therefore energetically accessible from the vertically formed cation radical.

An alternative, and energetically more favorable, pathway starts from $2b^{+\bullet}$, which is 9 kJ mol⁻¹ more stable than $2a^{+\bullet}$ and can be formed either directly upon electron transfer to 2^{2+} followed by geometry relaxation or by isomerization of $2a^{+\bullet}$.

(46) (a) Williams, B. W.; Porter, R. F. *J. Chem. Phys.* **1980**, *73*, 5598–5604. (b) Gellene, G. I.; Cleary, D. A.; Porter, R. F. *J. Chem. Phys.* **1982**, *77*, 3471–3477. (c) Gellene, G.; Porter, R. F. *Acc. Chem. Res.* **1983**, *16*, 200–207. (d) Shaffer, S. A.; Tureček, F. *J. Am. Chem. Soc.* **1994**, *116*, 8647–8653. (e) Nguyen, V. Q.; Sadílek, M.; Frank, A. J.; Ferrier, J. G.; Tureček, F. *J. Phys. Chem. A* **1997**, *101*, 3789–3799. (f) Yao, C.; Tureček, F. *Phys. Chem. Chem. Phys.* **2005**, *7*, 912–920. (g) Boldyrev, A. I.; Simons, J. *J. Chem. Phys.* **1992**, *97*, 6621–6627.

Table 3. Dissociation and Transition State Energies for (GK + 2H)²⁺ Cation Radical **2a**²⁺

species/reaction	relative energy ^{a,b}	
	B3LYP/ 6-31++G(d,p)	B3-PMP2/ 6-311++G(2d,p)
1 ²⁺ → 2a ²⁺	−71	−90
2a ²⁺ → 2b ²⁺	−9	−9
2a ²⁺ → 2c ²⁺	50	46
2a ²⁺ → 2d ²⁺	11	12
2a ²⁺ → TS14	60	60
2a ²⁺ → TS15	55	59
2a ²⁺ → 2e ²⁺	−21	−11
2a ²⁺ → TS16	−15	−12
2a ²⁺ → 2f ²⁺	−24	−17
2a ²⁺ → TS17	−17	−3
2a ²⁺ → 2g ²⁺	−131	−123
2a ²⁺ → c1 + z1 ²⁺	−9	0
2a ²⁺ → TS18	94	90
2a ²⁺ → 2h ²⁺ + H ⁺	63	43
2a ²⁺ → TS19	112	117
2a ²⁺ → 2i ²⁺	49	58

^a In units of kJ mol^{−1}. ^b From B3-PMP2/6-311++G(2d,p) single-point calculations including B3LYP/6-31++G(d,p) zero-point vibrational energies.

Although **2b**²⁺ is a local potential energy minimum, the inductive effect of the unpaired electron in the Lys radical moiety increases the basicity of the Gly amide group and results in a practically barrierless (**TS16**) proton migration from the Gly ammonium to the amide, forming intermediate **2f**²⁺, which is 8 kJ mol^{−1} more stable than **2b**²⁺ (Scheme 7). N—C_α cleavage in **2f**²⁺ proceeds through a low-energy transition state (**TS17**, 14 kJ mol^{−1} above **2f**²⁺) to form another ion–molecule complex (**2g**²⁺). Note (Table 3) that **2g**²⁺ is substantially more stable than **2e**²⁺ and also has the correct charge distribution, as it contains a protonated Lys fragment. Thus, **2g**²⁺ directly correlates with the expected products, which are a neutral **c1** fragment and the **z1**²⁺ ion. The overall dissociation is practically thermoneutral when referenced to **2a**²⁺ (Table 3).

The spontaneous isomerization to **2a,b**²⁺ upon electron transfer, followed by low-energy isomerizations, directs the dissociation of charge reduced **2**²⁺ toward N—C_α bond cleavage and formation of **c** and **z**²⁺ fragments. The calculations indicate that the products may be formed by more than one mechanism. We have also investigated the possibility for a radical-induced H atom loss or a Lys side-chain loss from some intermediates (Scheme S1). However, dissociation of the O—H bond in **2b**²⁺ has a high activation energy (**TS18**, Table 3), and the overall loss of H to produce a zwitterionic form of (GK + H)⁺ (**2h**²⁺) is endothermic. Likewise, cleavage of the C_α—C_β bond in **2b**²⁺ requires a high activation energy (**TS19**, Table 3) to form ion-radical complex **2i**²⁺. We conclude that loss of an H atom from **2b**²⁺ is disfavored and should not compete with the N—C_α bond cleavage and formation of **z**²⁺ ions.

(KK + 2H)²⁺ Ion Structures and Relative Stabilities. Several tautomers and conformers were investigated for (KK + 2H)²⁺ cations to establish the order of relative stabilities and isomer populations in the gas phase. As with (GK + 2H)²⁺, the conformer stabilities are mainly determined by two factors, one being the Coulomb repulsion between the charged groups and the other the charge–dipole and dipole–dipole attractions leading to intramolecular hydrogen bonding. The optimized structures of ions **7**²⁺–**15**²⁺ are shown in Figure 6, and their relative enthalpies and free energies at 298 K are summarized in Table 4. Conformer **7**²⁺ is the thermochemically most stable structure, which has the C-terminal lysine ammonium group

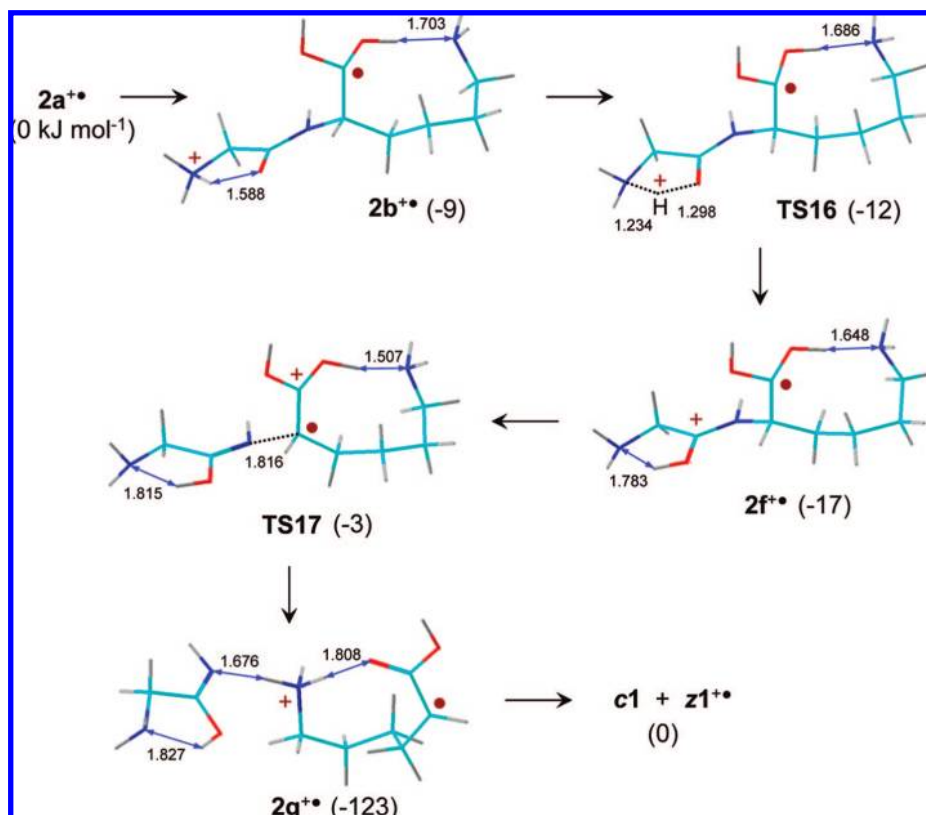
hydrogen bonded to the carboxyl group, and the N-terminal lysine ammonium is hydrogen bonded to the amide carbonyl and free amino group. The conformation and hydrogen bonding of the N-terminal lysine side chain in **7**²⁺ closely resemble those in the most stable conformer of protonated lysine.⁴⁷ The second most stable conformer (**8**²⁺) has the same conformation of the C-lysine part as does **7**²⁺, but the N-terminal lysine shows only one H-bond to the amino group. The less constrained N-terminal lysine side chain in **8**²⁺ results in a higher entropy compared to that in **7**²⁺. Consequently, **8**²⁺ has the lower ΔG_{g,298}^o of the two conformers and is thermodynamically the most stable structure albeit only by a small margin (Table 4). Conformers **9**²⁺, **10**²⁺, and **11**²⁺ that have unfolded C-terminal lysine residues are 18–24 kJ mol^{−1} less stable than **7**²⁺. The increase of entropy upon unfolding the lysine side chain lowers the relative ΔG_{g,298}^o of **9**²⁺, **10**²⁺, and **11**²⁺ by 4–8 kJ mol^{−1} but does not lead to a reversal of relative thermodynamic stabilities. The relative ΔG_{g,298}^o for the five thermodynamically most stable conformers **8**²⁺, **7**²⁺, **9**²⁺, **11**²⁺, and **10**²⁺ indicate their equilibrium populations at 298 K to be 67, 30, 2, 0.6, and 0.04%, respectively. Structures were also optimized for several other isomers, e.g., **12**²⁺–**15**²⁺ (Figure 6). All these conformers were substantially less stable than **7**²⁺ and **8**²⁺ (Table 4) and are not expected to be significantly populated at gas-phase equilibrium. It can be concluded that **7**²⁺ and **8**²⁺ are the major precursor ion species that are expected to coexist at equilibrium in the gas phase and are accompanied by **9**²⁺ and **11**²⁺ as minor components. This implies that (KK + 2H)²⁺ cation radicals formed by collisional electron transfer consist of two major populations whose reactivities and interconversions must be studied in order to describe the dissociations.

(KK + 2H)²⁺ Cation Radicals. Electron attachment to **7**²⁺ and **8**²⁺ is associated with vertical recombination energies of RE_{vert} = 4.95 and 4.80 eV, respectively (Table 5). However, structures **7**²⁺ and **8**²⁺ are not local energy minima. The initially formed species spontaneously rearrange by barrierless migration of a hydrogen from the C-terminal lysine ammonium to the carboxyl group, forming isomers **7a**²⁺ and **8a**²⁺, respectively (Scheme 8). In addition, the isomerization in **8a**²⁺ also involved a migration of the N-terminal lysine proton onto the α-amino group. **7a**²⁺ is found to be more stable both thermochemically and thermodynamically than **8a**²⁺ (Table 5). The adiabatic recombination energies for **7**²⁺ + e[−] → **7a**²⁺ and **8**²⁺ + e[−] → **8a**²⁺, which include the change of energy upon rearrangement, were calculated as 6.36 and 6.12 eV, respectively (Table 5). These indicate that upon combined resonant electron transfer from Na and rearrangement, cation radicals **7a**²⁺ and **8a**²⁺ receive 6.36 − 5.14 = 1.22 eV (118 kJ mol^{−1}) and 6.12 − 5.14 = 0.98 eV (95 kJ mol^{−1}) energy in the form of vibrational excitation. From the heat capacities of **7a**²⁺ and **8a**²⁺ and the energy deposited upon electron transfer and isomerization, we estimate the effective vibrational temperature of **7a**²⁺ and **8a**²⁺ to be about 470 K. The difference in free energy, ΔG_{g,470}^o(**7a**²⁺ → **8a**²⁺) = 10.6 kJ mol^{−1}, indicates 94% of **7a**²⁺ at equilibrium.

To address the question of whether the **8a**²⁺ → **7a**²⁺ isomerization was kinetically feasible, we mapped by B3LYP calculations the potential energy surface for the rearrangement

(47) (a) Bleiholder, C.; Suhai, S.; Paizs, B. *J. Am. Soc. Mass Spectrom.* **2006**, *17*, 1275–1281. (b) Bush, M. F.; Forbes, M. W.; Jockusch, R. A.; Oomens, J.; Polfer, N. C.; Saykally, R. J.; Williams, E. R. *J. Phys. Chem. A* **2007**, *111*, 7753–7760. (c) Vaden, T. D.; De Boer, T. S. J. A.; MacLeod, N. A.; Marzluff, E. M.; Simons, J. P.; Snoek, L. C. *Phys. Chem. Chem. Phys.* **2007**, *9*, 2549–2555.

Scheme 7



of hydrogen bonds in the protonated N-terminal lysine chain and located the transition state. The activation energy for the rearrangement, $E_{TS} = 8 \text{ kJ mol}^{-1}$ relative to $8a^{2+}$ from single-point B3-MP2 calculations, is negligible with respect to the vibrational excitation in the cation radical and indicates very fast conformational rearrangement in $8a^{2+}$ following electron transfer.

Electron transfer to the minor cation 9^{2+} is associated with $RE_v = 5.20 \text{ eV}$ (Table 5) and results in the formation of cation radical 9^{+} , which is a local energy minimum. However, 9^{+} is 94 kJ mol^{-1} less stable than $7a^{+}$ and presumably can dissociate by loss of an ammonium H atom or rearrange to $7a^{+}$ by facile side chain rotation similar to that described for $2a^{2+}$ and $2b^{2+}$.

(KK + 2H)⁺⁺Cation Radical Dissociations. N–C $_{\alpha}$ bond dissociations were investigated for $7a^{+}$ and $8a^{+}$, and the pertinent transition states were located as **TS20** and **TS21** (Scheme 8). In both transition states, the reaction coordinate consists of a coupled motion separating the amide N and C $_{\alpha}$ atoms, combined with a migration of the carboxyl proton onto the C-terminal lysine amino group. The activation energies for the N–C $_{\alpha}$ bond dissociations are comparable when starting from $7a^{+}$ ($E_a = 40 \text{ kJ mol}^{-1}$) and $8a^{+}$ ($E_a = 39 \text{ kJ mol}^{-1}$), which places **TS20** 14 kJ mol^{-1} below **TS21** (Table 5). Both N–C $_{\alpha}$ bond dissociations lead to intermediates, $7b^{+}$ and $8b^{+}$, respectively, which are 24 and 27 kJ mol^{-1} higher in energy than the respective reactants. Intermediate $7b^{+}$ is an ion–molecule complex of a distonic isomer of the lysine cation radical originating from the C-terminal lysine residue and a neutral enolimine originating from the N-terminal lysine residue. $8b^{+}$ is an ion–molecule complex in which the N-terminal Lys residue is a zwitterion. This assignment is substantiated by the pertinent atomic electron densities which are described and discussed in the next section. The calculated TS energies indicate

very facile N–C $_{\alpha}$ bond dissociations in $(\text{KK} + 2\text{H})^{++}$ cation radicals, in keeping with TS energies reported previously for other neutral and charged peptide models.^{16–21} Interestingly, the conformation and H-bonding framework of the N-terminal residue have a very small effect on the activation energies for the N–C $_{\alpha}$ bond cleavages, indicating that the transition state energies are mainly determined by interactions between the unpaired electron in the dihydroxymethyl radical and those in the dissociating N–C $_{\alpha}$ bond.

The ion–molecule complexes $7b^{+}$ and $8b^{+}$ can separate into c and z^{+} fragments, which require 87 kJ mol^{-1} relative to $7a^{+}$ at the thermochemical threshold (Table 5). This potential energy barrier is less than the internal energy provided by vertical electron transfer from Na (118 kJ mol^{-1} , vide supra), and so $7a^{+}$ is metastable with respect to this dissociation. However, the system can follow an energetically more favorable pathway that involves exothermic proton transfer between the incipient c and z^{+} fragments to form stable ion molecule complexes $7c^{+}$ and $7d^{+}$ (Scheme 9). The former can dissociate to a neutral z^{\bullet} fragment and a c^{+} fragment, which can be either the protonated enolimine 17^{+} or the more stable protonated lysine amide 18^{+} (Scheme 9). The formation of the most stable $c^{+} + z^{\bullet}$ pair is 9 kJ mol^{-1} exothermic relative to $7a^{+}$ at the thermochemical threshold of dissociation. Given the extremely low threshold energy and the substantial internal energy acquired by $7a^{+}$ upon electron transfer from Na, it is understandable that the charge reduced peptide ion dissociates rapidly so that no survivor ion is detected on the microsecond time scale of the ECID experiment.²⁶

Electron Density Distribution in (KK + 2H)⁺⁺ Cation Radicals, Transition States, and Dissociation Products. The charge distribution in the fragments formed by N–C $_{\alpha}$ bond dissociation is known from the ECID spectrum to favor the c

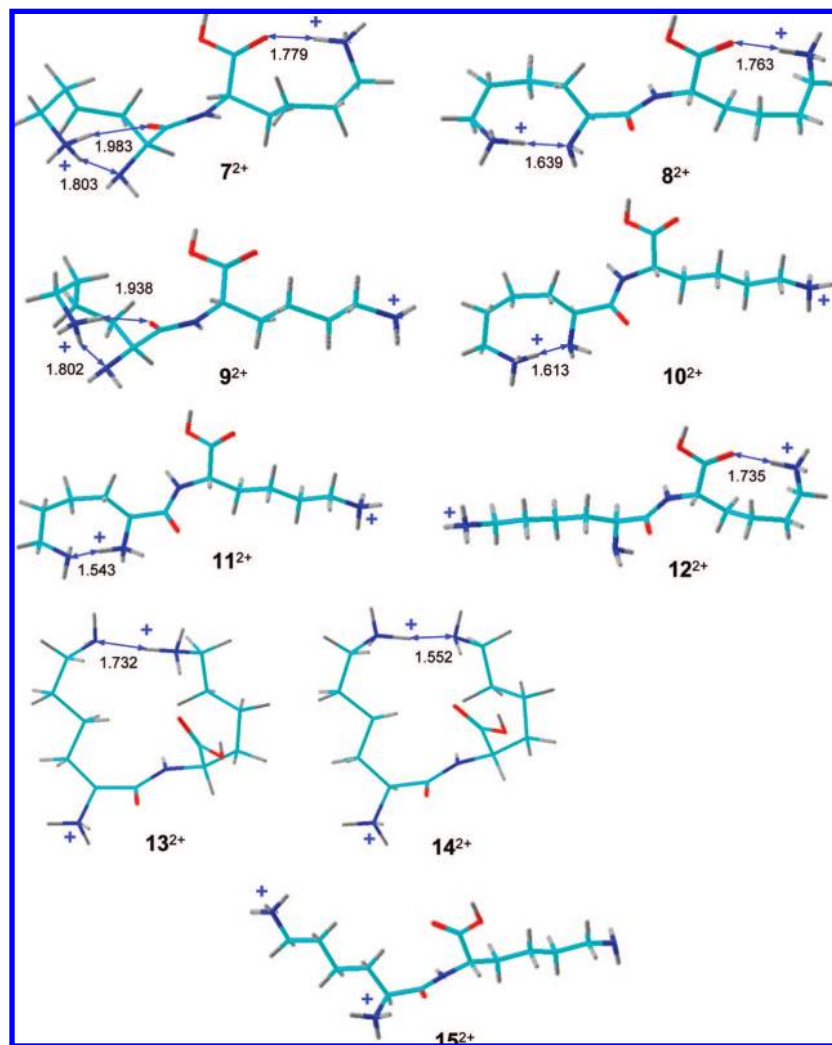


Figure 6. B3LYP/6-31+G(d,p) optimized structures of $(\text{KK} + 2\text{H})^{2+}$ cations 7^{2+} – 15^{2+} .

Table 4. Relative Energies of $(\text{KK} + 2\text{H})^{2+}$ Cations 7^{2+} – 15^{2+}

conformer	relative energy ^{a,b}	
	B3LYP/ 6-31+G(d,p)	B3-MP2/ 6-311++G(2d,p)
7^{2+}	–1.8	–5.0 (2.0) ^b
8^{2+}	0.0	0.0 (0.0) ^b
9^{2+}	18	13 (9) ^b
10^{2+}	21	20 (12) ^b
11^{2+}	24	24 (19) ^b
12^{2+}	35	32
13^{2+}	67	54
14^{2+}	82	70
15^{2+}	150	–

^a Relative enthalpies in units of kJ mol^{-1} including B3LYP/6-31+G(d,p) zero-point energy corrections and 298 K enthalpies.

^b Values in parentheses are relative free energies at 298 K.

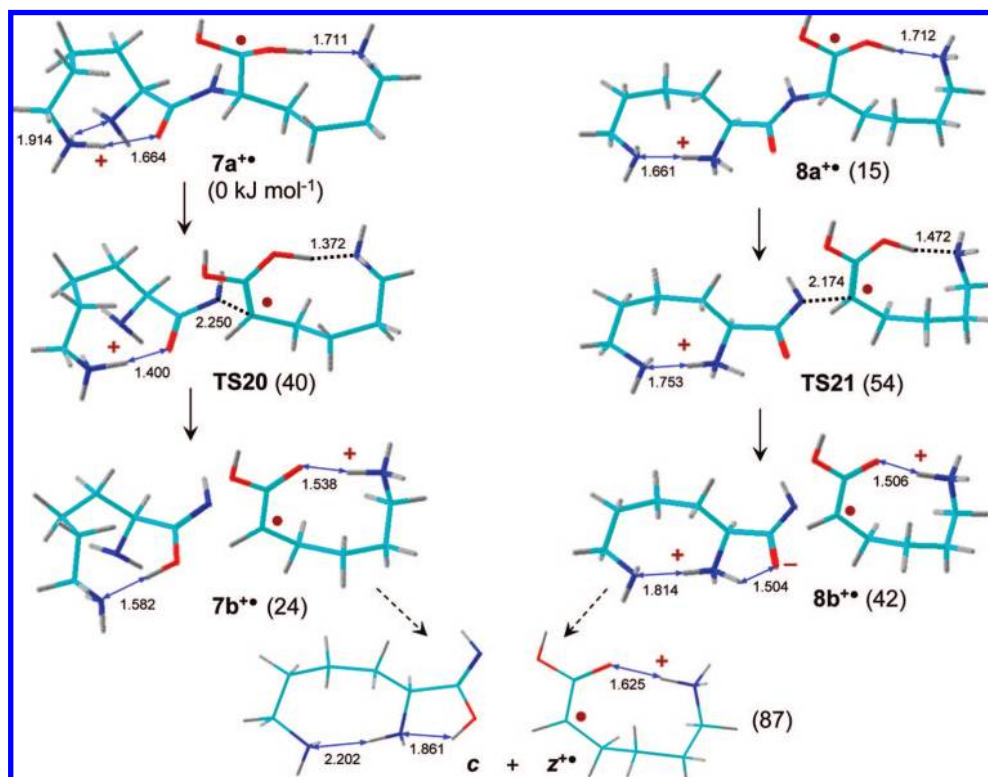
ion over the z ion in a ca. 8:1 ratio. It is instructive to follow the charge distribution along the entire ECID process starting with vertical electron transfer and including the rearrangements, transition states, ion–molecule complexes, and final dissociation products. Because of the similarity between the behaviors of 7a^{++} and 8a^{++} , we will mainly discuss the path involving the latter isomer. The path for 7a^{++} was also investigated and found to be quite analogous to that for 8a^{++} .

Table 5. Relative Energies of $(\text{KK} + 2\text{H})^{++}$ Cation Radicals

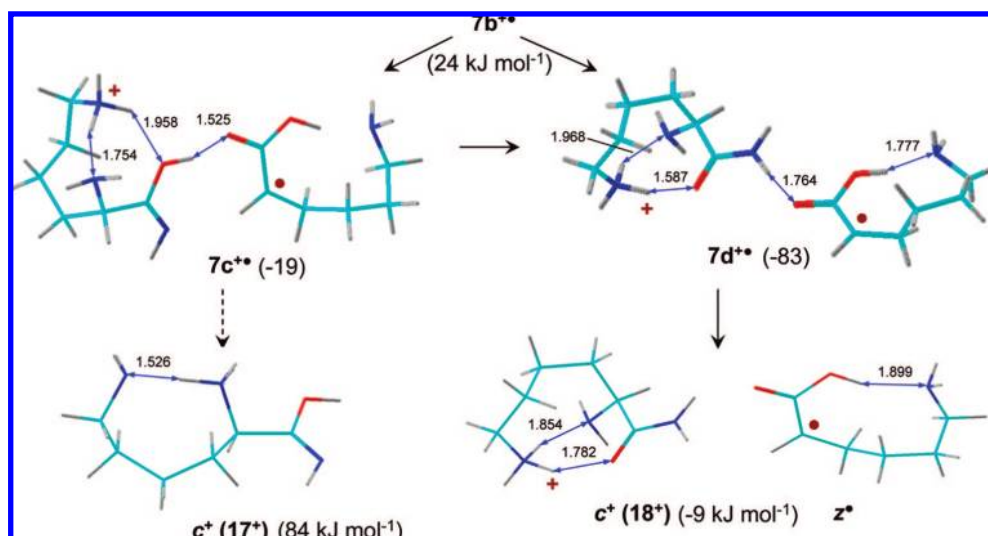
species/reaction	relative energy ^a	
	B3LYP/ 6-31++G(d,p)	B3-MP2/ 6-311++G(2d,p)
$7^{2+} \rightarrow 7^{++}$	–506	–478 (4.95) ^c
$8^{2+} \rightarrow 8^{++}$	–496	–463 (4.80) ^c
$7^{2+} \rightarrow 7\text{a}^{++}$	–628	–614 (6.36) ^d
$8^{2+} \rightarrow 8\text{a}^{++}$	–604	–591 (6.12) ^d
$9^{2+} \rightarrow 9^{++}$	–554	–502 (5.20) ^c
		–538 (5.57) ^d
$7\text{a}^{++} \rightarrow 8\text{a}^{++}$	12	15 (11) ^b
$7\text{a}^{++} \rightarrow 9^{++}$	93	94
$7\text{a}^{++} \rightarrow \text{TS20}$	28	40
$8\text{a}^{++} \rightarrow \text{TS21}$	28	39
$7\text{a}^{++} \rightarrow 7\text{b}^{++}$	19	24
$8\text{a}^{++} \rightarrow 8\text{b}^{++}$	20	27
$7\text{a}^{++} \rightarrow \text{c} + \text{z}^{++}$	76	87
$7\text{a}^{++} \rightarrow \text{c}^+(17^+) + \text{z}^{\cdot}$	70	84
$7\text{a}^{++} \rightarrow \text{c}^+(18^+) + \text{z}^{\cdot}$	–22	–9
$8\text{a}^{++} \rightarrow 8\text{d}^{++}$	–91	–80
$7\text{a}^{++} \rightarrow 7\text{c}^{++}$	–27	–19
$7\text{a}^{++} \rightarrow 7\text{d}^{++}$	–96	–83
$7\text{a}^{++} \rightarrow \text{TS22}$	121	120
$7\text{a}^{++} \rightarrow 19^+ + \text{H}^{\cdot}$	80	61

^a Relative enthalpies in kJ mol^{-1} including B3LYP/6-31++G(d,p) zero-point energy corrections and referring to 0 K unless stated otherwise. ^b Relative free energy at 298 K. ^c Vertical recombination energies in eV. ^d Adiabatic recombination energies in eV.

Scheme 8



Scheme 9



Vertical electron attachment to 8^{2+} forms a transient point on the potential energy surface of the X state which is described by the manifold of electronic states shown in Figure 7. The X state has the unpaired electron in a diffuse orbital consisting of a 3s Rydberg-like orbital at the N-terminal lysine ammonium, which is in a bonding combination with a 3s Rydberg-like orbital at the C-terminal lysine ammonium and a carboxyl π^* orbital. The atomic spin densities from NPA analysis indicate 61% of unpaired spin density at the C-lysine residue and 39% at the N-terminal one. The atomic charge distributions are similar, e.g., 60/40 for the C and N terminal lysines. Thus, the initial species has the unpaired electron delocalized over orbitals covering both amino acid residues. This again suggests that *the electron cannot be localized at any particular former charge site*. Similar

conclusions follow from the wave functions of the low-lying excited states that may be accessed by electron transfer. For example, the A state is described by a destructive superposition of the spatially remote 3s Rydberg-like orbitals at the N- and C-terminal lysine ammonium groups but has practically no electron density at the carboxyl group. The B state is a combination of a C-terminal lysine ammonium Rydberg-like orbital and a carboxyl π^* orbital but has negligible electron density in the N-terminal lysine ammonium. The C and E states are combinations of carboxyl and amide π^* orbitals, while the D state is mainly represented by a 3p Rydberg-like orbital at the N-terminal ammonium.

In spite of electron delocalization, the reactivities of the former charge sites dramatically differ in particular electronic

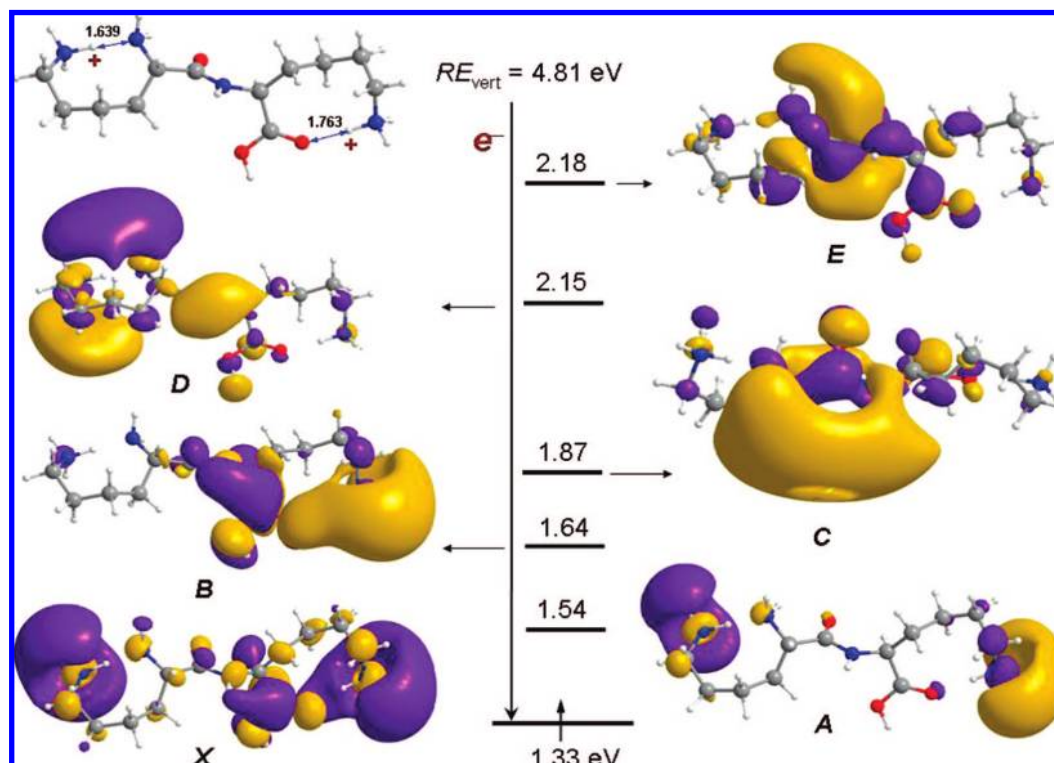


Figure 7. Electronic states in vertically reduced 8^{++} . The energies (eV) are relative to the ground (X) state. The molecular orbitals are shown as in Figure 3.

states. When the 8^{++} system is allowed to relax on the potential energy surface of the X state, it follows a downward trajectory leading to a new structure $8a^{++}$, which develops a very different electronic structure. The X state in $8a^{++}$ is a π orbital of the dihydroxymethyl radical, where 94% of the unpaired electron density is localized in the HO–C–OH group. The excited electronic states in $8a^{++}$ are ≥ 2.6 eV above the X state and do not overlap by energy with the low excited states of vertically formed 8^{++} . Thus, the low excited states in 8^{++} can correlate only with the ground electronic state of $8a^{++}$.

The potential energy surfaces for the excited states accessed by vertical electron transfer in 8^{++} were not mapped but can be estimated by analogy with those of alkyl ammonium and amino acid radicals for which detailed calculations have been reported.^{46f,g} For example, the A state in 8^{++} is expected to undergo dissociation of an N–H bond, which is known to have a very low activation energy^{46f,g} and will result in the loss of an H atom, as observed in the ECID spectra.²⁶ Although the previous experiments did not distinguish hydrogen atom losses from the ammonium groups in $(KK + 2H)^{++}$,²⁶ the odd-electron distribution in the A state indicates that loss from either group should be competitive. The B state of 8^{++} is expected to rearrange to $8a^{++}$, due to the interaction between the ammonium and COOH orbitals (Figure 7). The C and E states have substantial electron density in the amide groups and are expected to be superbasic¹⁸ and exothermically capture a proton from one of the ammonium groups.

The electron distribution in **TS20** and **TS21** shows 73% of spin density in the C-lysine residue, which also holds 65–68% of atomic charge. This indicates that in the early stages of dissociation the TS develops into a C-terminal lysine cation radical where the N-terminal lysine part carries a minor portion of the total positive charge. This is even more pronounced in ion–molecule complexes $8b^{++}$ and $7b^{++}$, which carry 85–93%

of unpaired electron density and 84–92% of positive charge in the C-terminal lysine residue, which is the incipient z^{++} fragment. Interestingly, the N-terminal lysine fragment is a neutral zwitterion which owes stabilization to the presence of the cation-radical z^{++} fragment in the complex. Evidently, the charge distribution in the TS and in the immediate ion–molecule complexes does not correspond to that in the separate fragments, which prefer c^+ over z^{++} , consistent with the calculated dissociation thermochemistry (see above). The ion–molecule complexes can get stabilized by exothermic proton transfer from the incipient z^{++} fragment to the c zwitterion. The proton transfer can form several ion–molecule complexes that differ in the protonation site on the N-lysine fragment (α - or ϵ -amino group) and whether they have an enolimine or amide functionality. The most stable complex we found ($7d^{++}$, Scheme 9) consists of an ϵ -protonated lysine amide and the z radical and is 83 kJ mol⁻¹ below $7a^{++}$ (Table 5). Which of the possible complexes is formed upon ECID of $(KK + 2H)^{++}$ cannot be established from our calculations; note, however, that the complexes completely dissociate on the microsecond time scale of the ECID experiment.

Discussion

The previous analysis revealed two major phenomena occurring upon electron capture in doubly protonated peptides. First, electron capture by the peptide ions can result in the formation of a multitude of closely spaced electronic states. The lowest states have the unpaired electron delocalized over remote ammonium and/or amide or carboxyl groups. In other words, the unpaired electron cannot be assigned to a particular localized orbital at a former charge site. This finding is in major contrast with conclusions drawn from the analysis of singly charged amide models, where the unpaired electron was placed in an isolated orbital of π or σ type representing a selected electronic state.²² Our finding of electron delocalization in GK, GGK, and

KK peptide cation radicals indicates that similar phenomena are likely to exist upon electron capture by larger peptide ions including those carrying multiple (>2) charges. The near-degeneracy of low electronic states and the ensuing electron delocalization is a phenomenon, which is particular to peptide cations and is due to the very similar intrinsic recombination energies of the charge-carrying groups. The degeneracy is removed in the presence in the peptide of a functional group with a substantially higher intrinsic recombination energy, in which case the electron is localized on that group in the ground electronic state. This has substantial effects on the ECD of such modified peptides, as reported recently for spin-trap capped peptides⁴⁸ and also for peptide-transition metal complexes.⁴⁹

Second, upon electron attachment, protonated C-terminal Lys residues are found to undergo spontaneous rearrangement by proton migration to the proximate carboxyl group that directs the further dissociation of the cation-radical intermediates. A major electronic effect of the rearrangement is that it removes the electronic state degeneracy by increasing the $X-A$ gap in the dihydroxymethyl cation-radical intermediate. In GK and KK peptides, the pertinent intermediates can undergo facile dissociations of $N-C_\alpha$ bonds adjacent to the Lys residue, which are combined with proton migrations between the incipient fragments. The charge distribution between the c and z fragments correlates with the product relative stabilities, not the charge distribution in the transition state of the $N-C_\alpha$ bond cleavage. This underlines the role of ion molecule complexes¹⁷ in which the energetically most favorable charge distribution can be readily achieved by low-energy proton migrations. An interesting question arises as to how to extrapolate the present results to explain dissociations of larger tryptic peptides where $N-C_\alpha$ bond cleavages occur at sites which are remote from the C-terminal residue. One possibility is that the dissociation occurs in a conformer in which the Lys ammonium group is H-bonded to a remote amide group of the peptide chain. Such a mechanism is analogous to those studied for the present dipeptides, because the pertinent dihydroxymethyl and aminoketyl intermediates are electronically alike and both substantially weaken the adjacent

$N-C_\alpha$ bonds. However, this mechanism does not explain $N-C_\alpha$ dissociations of bonds that are spatially remote in charge-reduced cation radicals.^{18,22} For such systems, an alternative mechanism has been suggested that involved electron capture in an excited state represented by an amide π^* orbital. Such states are bound in the presence of an additional charge in the peptide cation radical and have energies that depend on the amide group distance from the remaining charge.^{18,22} The present $(GK + 2H)^+$, $(GGK + 2H)^+$, and $(KK + 2H)^+$ cation radicals have the peptide amide group very close to the charged ammonium groups, and thus the pertinent amide π^* states have low excitation energies. Analysis of excited-state potential energy surfaces in cation radicals derived from doubly protonated tripeptides, and larger systems will be needed to reveal the mechanistic details of competing $N-C_\alpha$ bond cleavages and to identify the reactive excited states.

Conclusions

Electron structure theory analysis of the potential energy surfaces of $(GK + 2H)^+$ and $(KK + 2H)^+$ cation radicals provides an explanation of competitive dissociations observed upon collisional electron transfer to gas-phase peptide ions. The doubly protonated peptides are found to consist of two major populations of gas-phase conformers forming distinct populations of cation radicals upon electron transfer. Electronic structure analysis of $(GK + 2H)^+$ and $(KK + 2H)^+$ conformers points to extensive delocalization of unpaired electron density over spatially remote ammonium, carboxyl, and amide groups in near-degenerate electronic states. This indicates that the model of charge localization in a particular group in the charge-reduced peptide is an oversimplification and that orbital interactions of remote groups over distances exceeding 13 Å should be taken into account in the analysis and discussions of dissociation mechanisms.

Acknowledgment. Support by grants from the National Science Foundation (CHE-0349595, CHE-0342956, and CHE-0750048) is gratefully acknowledged. F.T. thanks Professors Steen Brøndsted Nielsen and Preben Hvelplund of the Department of Physics and Astronomy, University of Aarhus, Denmark, for stimulating discussions of electron capture induced dissociations during his stay at University of Aarhus in June–August 2007.

Supporting Information Available: Complete ref 28, Tables S1–S51 with optimized geometries in standard orientation, Figure S1, and Scheme S1. This information is available free of charge via the Internet at www.pubs.acs.org.

JA8019005

- (48) (a) Belyayev, M. A.; Courmoyer, J. J.; Lin, C.; O'Connor, P. B. *J. Am. Soc. Mass Spectrom.* **2006**, *17*, 1428–1436. (b) Jones, J. W.; Sasaki, T.; Goodlett, D. R.; Tureček, F. *J. Am. Soc. Mass Spectrom.* **2007**, *18*, 432–444.
- (49) (a) Fung, Y. M. E.; Liu, H.; Chan, T.-W. D. *J. Am. Soc. Mass Spectrom.* **2006**, *17*, 757–771. (b) Adamson, J. T.; Hakansson, K. *Anal. Chem.* **2007**, *79*, 2901–2910. (c) Liu, H.; Hakansson, K. *J. Am. Soc. Mass Spectrom.* **2006**, *17*, 1731–1741. (d) Liu, H.; Hakansson, K. *Anal. Chem.* **2006**, *78*, 7570–7576. (e) Kleinnijenhuis, A. J.; Mihalca, R.; Heeren, R. M. A.; Heck, A. J. R. *Int. J. Mass Spectrom.* **2006**, *253*, 217–224.